MINERAL PARAGENESIS OF THE GRANULITE FACIES IN THE LAKE GEORGE AREA, NEW YORK

Abstract of

a thesis presented to the Faculty

of the State University of New York

at Albany

in partial fulfillment of the requirements

for the degree of

Master of Science

College of Science and Mathematics

Department of Geological Sciences

Boknam Ree

1991

ABSTRACT

The Lake George Area belongs to the southeastern part of the Adirondack Highlands. The rocks of this area show variations in mineral assemblages which are caused by differences in bulk chemical composition. This makes it unsuccessful to use a subdivision of the granulite facies which is suggested by de Waard (1965).

The CFM diagram (Abbott, 1982) is used to show the relationship between composition and paragenesis of the Lake George Area. In this study, a different result has been found in the order of partitioning of Fe between coexisting minerals, namely, garnet>hornblende>biotite≥orthopyroxene>clinopyroxene. The hornblende granitic gneiss belongs to a different subfacies from the mafic granulite and charnockitic gneiss according to Abbott's subdivision of the facies. But, following the order of X_{Fe} of the minerals from this study, the typical mineral assemblage of this rock, hornblende-garnet-biotite, may belong to the same subfacies as the other rock types of this area. The study of biotites of metapelite in the Lake George Area indicates different substitution mechanisms in different regions of the granulite facies.

From the garnet-orthopyroxene (clinopyroxene) thermometer, 710°C was obtained for the highest estimate of the metamorphism. This temperature condition appears to be consistent with the observed mineral assemblages of a lower-grade part of the granulite facies and confirms the isotherm pattern of Bohlen et al. (1985).

Cooling ages of 971±17 Ma, 882±7 Ma and 656±17 Ma were obtained for hornblende, biotite and microcline, respectively, with $^{40}Ar/^{39}Ar$ dating method. With cooling ages of minerals and reasonable closure temperatures for each mineral, average cooling rates are calculated: 2.7°C/Ma for the time interval of peak metamorphism-hornblende, 2.2°C/Ma for hornblende-biotite, and 0.7°C/Ma for biotite-microcline.

MINERAL PARAGENESIS OF THE GRANULITE FACIES IN THE LAKE GEORGE AREA, NEW YORK

A thesis

presented to the Faculty

of the State University of New York

at Albany

in partial fulfillment of the requirements

for the degree of

Master of Science

College of Science and Mathematics

Department of Geological Sciences

Boknam Ree

1991

ACKNOWLEDGMENTS

I am grateful to Dr. A. Miyashiro for providing this subject and financial support , and helpful discussions throughout the project. I would like to thank the other members of my thesis committee, Drs. G. W. Putman and W. S. Kidd for their reviews and helpful comments on the manuscript. I also thank Dr. W. D. Means for giving me a chance to study at Albany.

Matt Heizler and Dave Wark are thanked for technical assistance with $^{40}Ar/^{39}Ar$ dating method and with microprobe analyses, respectively. I am indebted to Dr. P. R. Whitney for lending some of his samples. I wish to acknowledge the rest of the faculty members and graduate students of the department for their support and help.

Diane Paton helped me in several ways to keep my thesis work flowing smoothly. Mrs. Yunmi Kim is specially thanked for spending a lot of time to take care of Hwisoo, my baby, while I wrote my thesis. I also thank my parents and parents-in-law for supporting me spiritually and financially. Finally, I thank Jin-Han Ree, my husband, for his encouragement and assistance with field work.

This thesis was supported by research Foundation 320-1586A to Akiho Miyashiro and State University of New York at Albany Benevolent Research grant.

TABLE OF CONTENTS

LIST OF TABLES

LIST OF FIGURES

CHAPTER 1. INTRODUCTION

1.1 Previous Studies

The Adirondack Mountains, New York, are made up of highly metamorphosed rocks which belong to the Allochthonous Monocyclic belt according to a new division of the Grenville Province (Rivers, et al., 1989). Geographically, it is divided into two parts, Adirondack Highlands and Lowlands. The Adirondack Lowlands are mostly composed of metasedimentary or migmatitic metasedimentary rocks. Whereas orthogneiss comprises a large part of the Adirondack Highlands.

There have been a lot of studies on the Adirondack Mountains since Buddington (1939, 1948). He was interested in the rocks associated with anorthosite and syenitic to granitic rocks in the Northwest Adirondacks and interpreted them as metamorphosed igneous rocks. In the 1950's and 1960's, detailed petrographic and mineralogical studies of the metamorphism of the Adirondacks were done by Engel and Engel (1958, 1960, 1962). Engel and Engel (1962) suggested that some of rocks which Buddington regarded as metamorphosed igneous rocks, were actually metamorphosed sedimentary rocks. With detailed mapping in the eastern and south-central Adirondacks, Walton and de Waard (1963) disclosed a "stratigraphic" sequence of Grenville metasedimentary rocks. They suggested that the Anorthosite might comprise a basement on which the Grenville sediments were later deposited, rather than intruding the metasedimentary rocks.

Buddington (1963) first recognized what he defined as isograds within the granulite facies terrain based on the presence and absence of garnet in the various rock types. Similar studies were done by de Waard (1965a, b, 1971). He attempted to subdivide the granulite facies with reference to variable P(load) - P(water) - T conditions with an help of the ACF diagram. De Waard (1965) confirmed Buddington's "second garnet isograd", but regarded the other garnet isograds as resulting from

"second garnet isograd", but regarded the other garnet isograds as resulting from differences in bulk chemical compositions. The significance of a garnet "isograd" in the granulite facies has been differently interpreted by Whitney (1978). He suggested that the garnet-producing reactions are retrograde, occurring during cooling from igneous temperatures.

With a paper on feldspar and oxide thermometry of granulites in the Adirondacks (Bohlen and Essene, 1977) as a starting point, Bohlen et al. (1985) synthesized the temperature and pressure structure of the Adirondacks (Bohlen, 1979, 1980; Bohlen et al., 1985). There is also an estimate of P-T condition using liquidus equilibria of the granitic system (Putman & Sullivan, 1979).

There have been many attempts to date the time of the metamorphism and igneous activity of the Adirondacks with various dating methods (Hills and Gast, 1964; Silver, 1969; Basu and Pettingill, 1982; Ashwal and Wooden, 1985). Also, cooling ages of the rocks in the Adirondacks were obtained by other workers (Heizler and Harrison, 1986; Onstott and Peacock, 1987; Mezger et al., 1989).

Evolution of the Grenville rocks in the Adirondacks was another issue. Polymetamorphism was supported by Valley (1985) over isobaric-cooling. Contrary to the clockwise Pressure-Temperature-time (P-T-t) path which is a typical interpretation of the granulite facies, an anticlockwise P-T-t path of metamorphism was suggested for the Adirondack Mountains (Bohlen, 1983, 1987). Earlier events before Grenville metamorphism are rather controversial.

Not much study has been done about the structural geology and stratigraphy in the present study area, but references can be given to McLelland and Isachsen (1980) and Wiener et al. (1984). Post orogenic history of the Adirondack Mountain region has been reviewed (Selleck, 1980).

1.2 The Object of this Study

There have been arguments about the distribution of metamorphic grades or temperatures in the Adirondacks since 1960's. Buddington (1963) and de Waard (1971) inferred isograds indicating an increase of metamorphic grade southeastward. Bohlen et al. (1977, 1985), in contrast, showed concentric isotherms around the Marcy anorthosite massif. Chemical exchange thermometry between two minerals like garnet-pyroxene has been widely used to infer pressure-temperature conditions in high grade metamorphic rocks. However, caution in the application of such thermometers to granulite facies rocks has been advised (Bohlen and Essene, 1980).

The aim of this paper is to test the two arguments about metamorphic temperature distribution in the Adirondack Mountains terrain. If de Waard is right, then temperature in the Lake George Area has to be the highest of the whole Mountains. In order to obtain pressure-temperature estimates of the metamorphism, various kinds of thermobarometers and calibrations have been tested. Several composition-paragenesis diagrams for metamorphosed rocks have been widely used for a better understanding of metamorphism. The AFM diagram (Thompson, 1957) is commonly applied to metapelitic rocks. It has not been as successful for use as a composition - paragenesis diagram for metamorphosed igneous rocks and mafic granulites. Consequently Abbott's CFM diagram (Abbott, 1982) is evaluated for such rocks in this region. The $^{40}Ar/^{39}Ar$ dating technique is very useful for revealing the cooling/uplifting history of crustal rocks, and has been applied to rocks of the Lake George Area in order to know this history after the major Grenville metamorphism.

1.3 Major Lithologic Units

The study area, referred to here as Lake George Area, is on the southeastern margin of the Highlands of the Adirondack Mountains, in which rocks have been considered as belonging to the granulite facies. Turner (1968) claimed that the Adirondacks are in transitional facies between upper amphibolite and granulite, which was termed the hornblende-granulite facies (Turner, 1958).

The Lake George Area is composed of metamorphosed igneous and metamorphosed sedimentary rocks. Figure 1-1 is a simplified geologic map of the Area. The locations of samples mentioned in this paper are shown in Fig. 1-2. Fisher (1984) classified the lithologies of the middle Proterozoic in the Glens Falls-Whitehall region into three groups: Metamorphosed igneous (plutonic) rocks, the Lake George Group (Metamorphosed sedimentary and igneous (volcanic) rocks), and the Piseco Lake Group. Detailed and lithology can be referred to Fisher (1984) and Wiener et al. (1984). In the following review, classification and description of the lithologies have been greatly simplified. Major rock types which are mentioned in the next chapter are briefly described here.

1.3.1 Metamorphosed igneous rocks

Olivine metagabbro, leucogranitic gneiss, hornblende granitic gneiss, magnetite ore beds, and metanorthosite belong to this group.

Olivine Metagabbros: Non-foliated, massive rock intruding other rock types. Best outcrop of intrusion into Hornblende Granitic Gneiss can be seen on the Prospect Mountain. This rock type is believed to be the youngest of the metamorphosed rocks.

Hornblende Granitic Gneisses: Because of the large mass of this rock type found at Prospect Mountain near the end of Lake George, in this study area it is called the Prospect Mountain Hornblende Granitic Gneiss (Fisher, 1984). Well-foliated hornblende

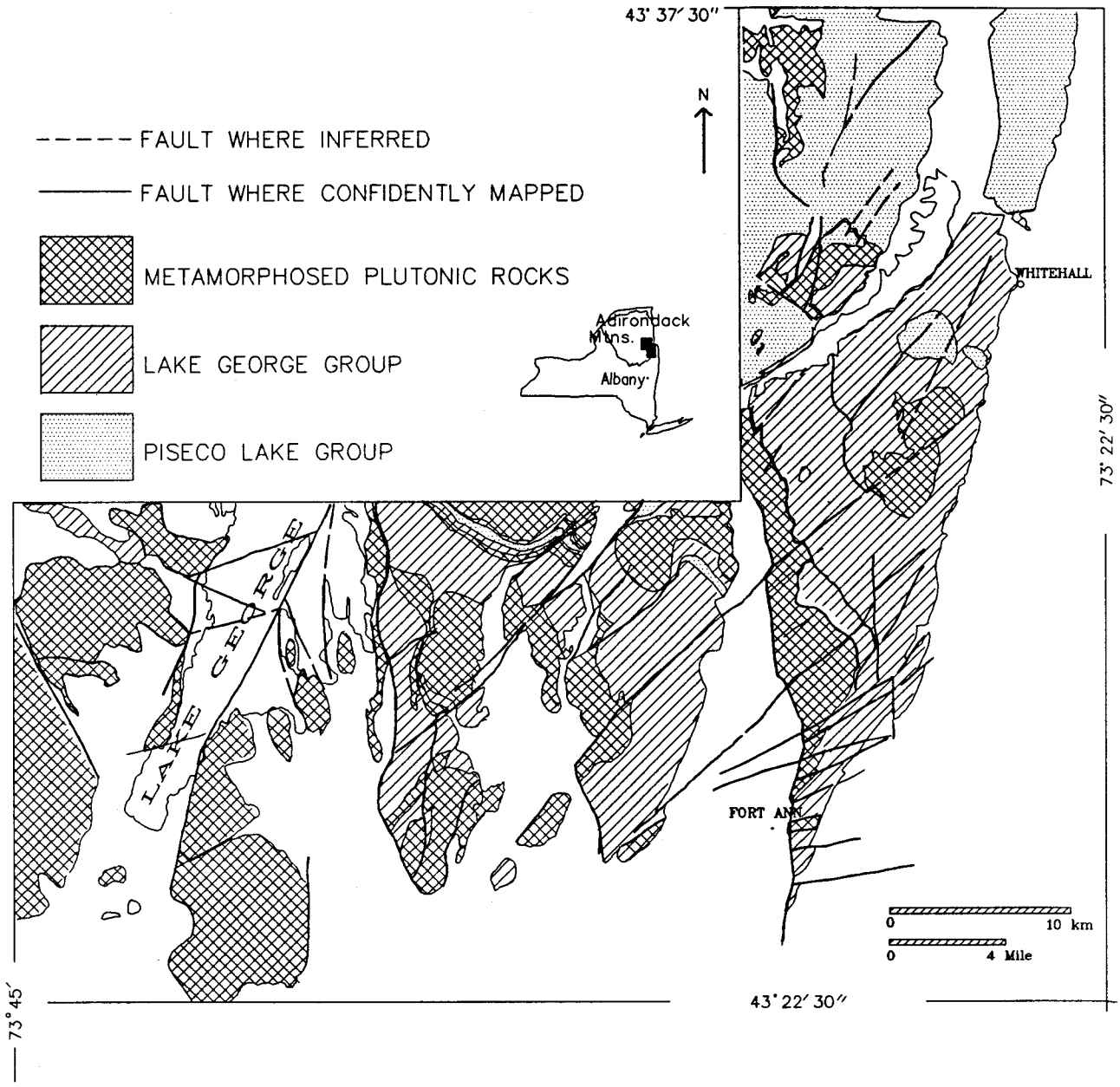

Fig. 1-1. The Precambrian lithologic map of the Lake George Area (after Fisher, 1984).

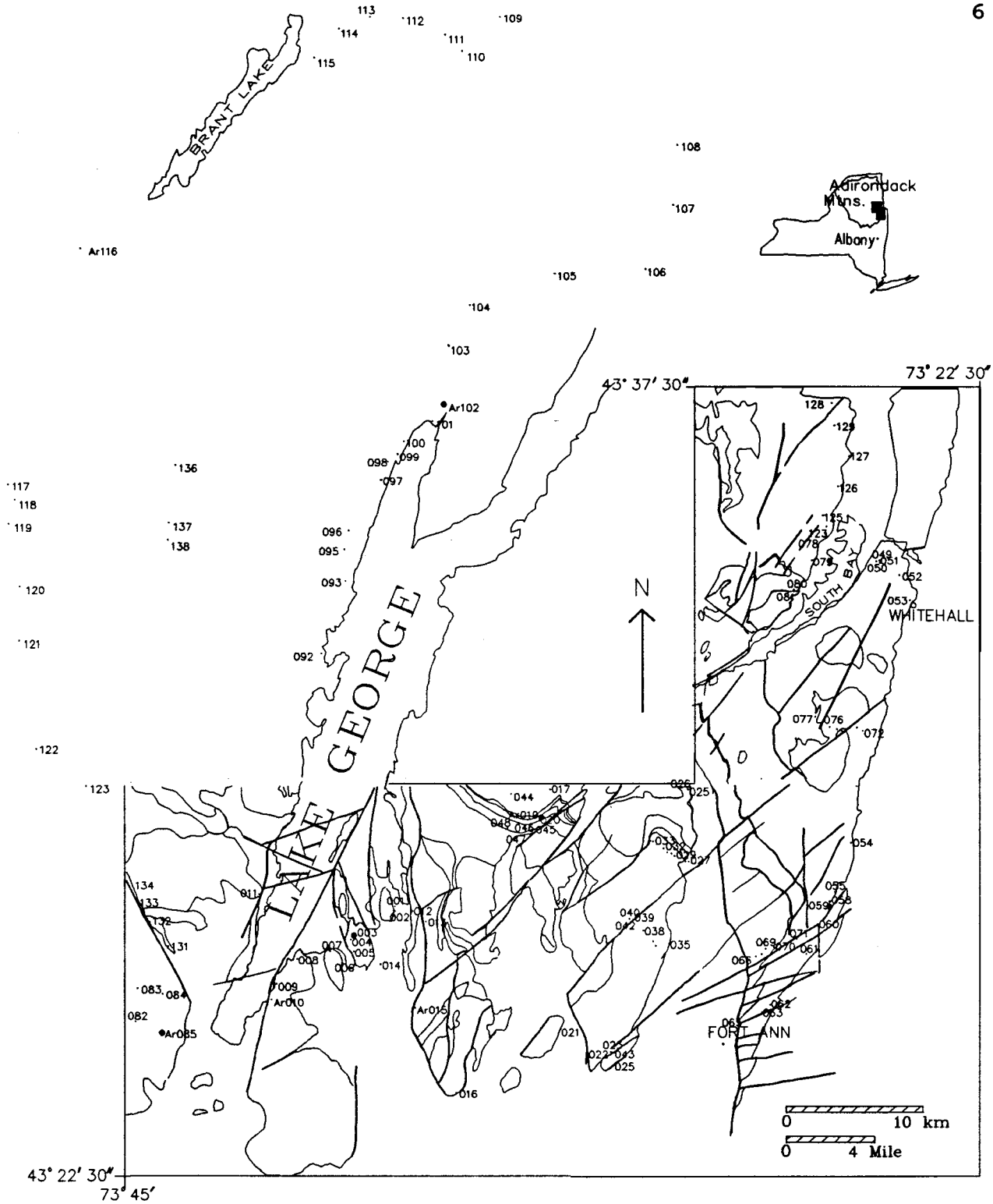

Fig. 1-2. A map showing the locations of samples which are mentioned in the text. Detailed geology is not available and samples are collected along the road in the northwestern area. Samples 019, 085, and 102 are used for Ar dating and 059 for the description in the section 2.3.

granitic gneiss shows pink to gray on weathered surface and is medium to coarse-grained.

1.3.2 Lake George Group

The Lake George Group includes sillimanite-biotite-garnet gneiss, biotite-quartz-plagioclase gneiss, marble, quartzite, and mafic granulites. Thin layers of amphibolite are interlayered with marble in this group.

Sillimanite-biotite-garnet Gneisses: These rocks are named the Hague gneiss and the Catamount sillimanite schist (Alling, 1918; Wiener, 1984). It is difficult to differentiate sillimanite-biotite-garnet gneiss from biotite-quartz-plagioclase gneiss, because sillimanite-biotite-garnet gneisses have the same mineral assemblages as biotite-quartz-plagioclase gneisses in many places.

Mafic Granulites: These rocks have been named the Beach Mountain Granulite and the Dresden Granulite (Alling, 1918) in the Thunderbolt Mountain Formation (Walton & de Waard, 1963) and the Paradox Lake Formation (Walton & de Waard, 1963), respectively, in the Lake George Group. They are weakly foliated and interlayered with other metasedimentary rocks.

1.3.3 Piseco Lake Group

The Piseco Lake Group, which has been claimed by some to be the basement complex of the Adirondack Mountains (Walton and de Waard, 1963; Wiener, et al., 1984), consists of the Pharaoh Mountain Gneiss (Wiener, et al., 1984) and overlying Brant Lake Gneiss (Bickford & Turner, 1971). The Pharaoh Mountain Gneisses as in a large exposure near Whitehall are interlayered charnockitic and granitic gneisses. They were grouped into two members (Fisher, 1984): Upper biotite-pyroxene member and Lower garnet-hornblende-pyroxene member (Fisher, 1984). This study failed to separate

one group from the other. They are bluish gray on fresh surface and strongly foliated. The Pharaoh Mountain Gneisses are called charnockitic gneiss in the next chapter.

CHAPTER 2. PARAGENESIS OF THE ROCKS IN THE LAKE GEORGE AREA.

2.1 Mineral assemblages and paragenetic types of the metamorphic facies.

The granulite facies was defined by Eskola (1939) for the rocks in which hydrous minerals are unstable and are replaced by anhydrous minerals like garnet, orthopyroxene and clinopyroxene. It is very common to have both kinds of minerals in the "so called" granulite facies rocks. Hornblende-granulite facies was suggested for the transition facies between upper amphibolite facies and granulite facies (Turner, 1958). The original granulite facies of Eskola was renamed the pyroxene-granulite facies.

De Waard (1965) proposed a division of the granulite facies according to P(water) - P(load) - T conditions. He divided the granulite facies into four subfacies (Fig. 2-1). P(water) - T controlled dehydration reactions separate the pyroxene-granulites from the hornblende-granulites. On the other hand, P(load) - T controlled anhydrous reactions separate the clinopyroxene-almandine subfacies from the orthopyroxene-plagioclase subfacies. It has been observed that rocks belonging to the different subfacies of de Waard occur in close proximity, even in a single outcrop. Since de Waard ignored solid-solution effects of minerals, his "subfacies" may not be true subfacies but represent only what this worker here calls "paragenetic type" which are produced by variations in bulk-rock compositions. The following will give some idea of the effect of bulk-rock compositions on mineral assemblages.

The transition from the upper amphibolite facies to the granulite facies is achieved by various dehydration reactions. The simplest reaction, for example, is the following:

$$K_2(Mg,Fe)_6Si_6Al_2O_{20}(OH)_4 + 6\ SiO_2 = 2\ KAlSiO_3 + 6\ (Mg,Fe)SiO_3 + 2\ H_2O \qquad (1)$$

Assuming biotite and orthopyroxene are Fe-Mg solid-solutions, the relationship between biotite and orthopyroxene is as shown in Fig. 2-2. In the present study, Mg/Fe ratios of

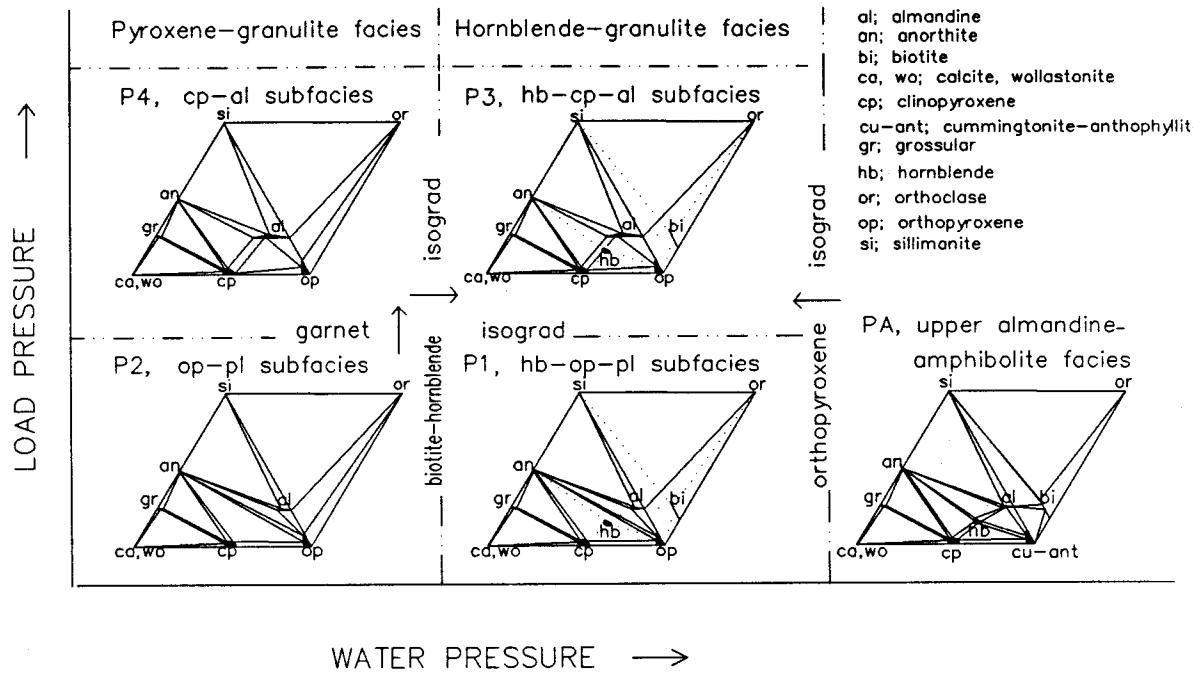

Fig. 2–1. Paragenetic types of the granulite facies based on de Waard's subdivision of the granulite facies.
Paragenetic types PA, P1, P2, P3 and P4 are given to each subfacies.

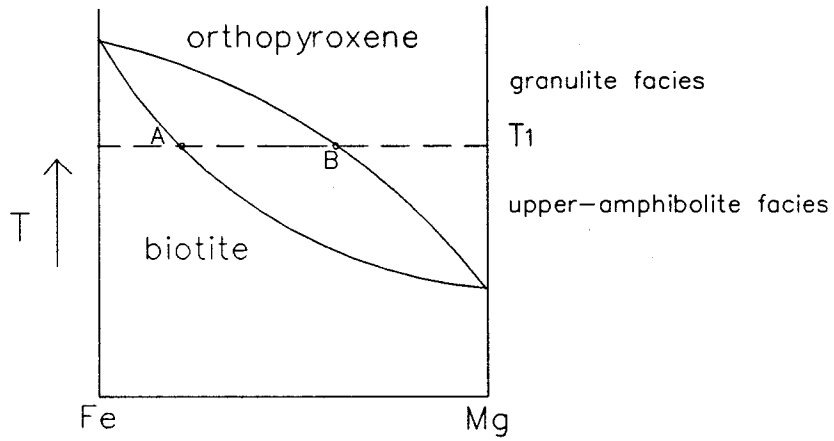

Fig. 2–2. Relationship between biotite and orthopyroxene in the presence of K–feldspar and quartz at a constant chemical potential of water. T1 is the temperature at the boundary to the granulite facies.

biotite and orthopyroxene are in similar ranges of value. Lonker (1980) shows that biotite has a higher Mg/Fe ratio than coexisting orthopyroxene in the granulite facies. However, a reverse relationship has been more frequently observed than that of Lonker in this study. Figure 2-2 is drawn according to the result of the present study. In the case of Fig. 2-2, if we define the granulite facies as a range of temperature above T_1, the granulite facies is characterized by biotite less magnesian than A in the presence of orthopyroxene, K-feldspar and quartz. Alternatively we may define the facies in terms of orthopyroxene of composition B. In orther words, the equilibrium temperature of a reaction like (1) varies with the composition of the relevant solid-solutions. Assuming that pressure, water pressure and temperature are uniform, Mg-rich rocks tend to show the assemblage of right-hand side of the reaction (1), where Fe-rich rocks tend to show assemblage of the left-hand side of that reaction. Therefore, for one type of metamorphic rocks at a single outcrop, they may show different mineral assemblages depending on the differences in Fe/Mg ratios of the rocks. In such a case, even though they have different mineral assemblages they are in the same metamorphic facies.

Another problem in de Waard's subdivision is that he used the ACF diagram. Unfortunately the ACF diagram failed to show the relationship between mineral paragenesis and Fe/Mg ratios and the effects of Na_2O and K_2O. Therefore de Waard's subdivision of the granulite facies, which is based on the topology of the ACF diagram, is incomplete and misleading.

By examination of thin sections under the microscope, various mineral assemblages can be found to define different "paragenetic types". In figure 2-1, each paragenetic type is represented by PA, P1, P2, P3, P4.

2.1.1 Hornblende Granitic Gneisses

A common mineral assemblage appearing in the Hornblende Granitic Gneiss is a quartz-plagioclase-K-feldspar-hornblende-(biotite)-garnet assemblage. The amount of

biotite in this rock type is small, that is, usually less than 3% in mode. Hornblende and garnet show alterations to chlorite. Clinopyroxene and orthopyroxene are observed in the mafic part of one thin section. Mineral assemblages for each sample are listed in Table I (a). Paragenetic types of the granulite facies are also indicated in that Table. Hornblende Granitic Gneisses fall mostly into PA and partly into P1.

2.1.2 Charnockitic Gneisses

These rocks were classified as the Piseco Lake Group in the previous chapter. Mineral assemblages of the Charnockitic Gneisses are shown in Table I (b). They belong to two paragenetic types of the granulite facies, P1 and P3 except for sample 067. They have two different mineral assemblages ; viz one has mainly biotite and pyroxene, the other has mainly garnet and hornblende rather than biotite.

2.1.3 Mafic Granulites

The presence of quartz in examples of this massive and dark granulite is variable. If there is quartz, then the amount will be very little. Garnet, clinopyroxene, orthopyroxene, hornblende, and biotite occur together. Table I (c) shows the mineral assemblages of mafic granulites. Their assemblages have been correlated to both P1 and P3 paragenetic types.

2.1.4 Olivine Metagabbros

Olivine metagabbro is believed to be the youngest of the metamorphosed rocks (Fisher, 1984). This rock shows well developed corona textures forming ellipsoidal or spherical shapes. The most common corona is formed by a reaction between olivine and plagioclase during metamorphism (Whitney, 1972; Whitney & McLelland, 1973; Whitney & McLelland, 1983). The original olivines are locally well preserved, elsewhere some are completely replaced by pyroxenes. The coronas usually consist of an olivine core

Table I. Tabulation of the mineral assemblages of the rocks in the Lake George Area.
+, observed to be present ; -, observed not to be present ; ?, not clear.

(a) Hornblende Granitic Gneisses

Sample No.	001	002	003-2	004-1	004-2	004-3	005	006	007	008	009	010	011	012	016	023	065
Biotite	x	x	x	x	x	-	x	x	x	x	x	x	x	x	x	x	x
Hornblende	x	x	x	x	x	x	x	x	x	x	x	x	x	x	x	x	x
Garnet	x	x	x	-	-	x	-	x	x	x	-	x	x	x	x	x	-
Orthopyroxene	-	-	-	-	-	-	x	?	-	-	-	-	-	-	-	-	-
Clinopyroxene	-	-	x	-	-	-	x	x	-	-	-	-	-	x	-	-	-
Paragenetic type	PA	PA	PA	PA	PA	PA	P1	P1	PA	PA	PA	PA	PA	PA	PA	PA	PA

(+ Quartz, + Plagioclase, + K-feldspar)

(b) Charnockitic Gneisses

Sample No.	062-2	108	067	079	107	060-3	120	124	125	127	129
Biotite	-	-	-	x	-	-	-	x	x	-	-
Hornblende	x	x	-	x	x	x	x	-	x	x	x
Garnet	x	x	x	-	x	-	x	-	x	-	-
Orthopyroxene	-	-	x	x	x	x	x	x	x	x	x
Clinopyroxene	x	x	x	x	x	x	x	x	x	x	x
Paragenetic type	P3	P3	P4	P1	P3	P1	P3	P1	P3	P1	P1

(+ Quartz + Plagioclase, + K-feldspar)

(c) Mafic Granulites

Sample No.	003-1	013	015	032	042	047	093-1	091	093-2	136	048	050-1	050-2	073	040	041
Plagioclase	x	x	x	x	x	x	x	x	x	x	x	x	x	x	x	x
K-feldspar	x	x	?	x	x	?	x	x	?	x	?	x	x	x	x	?
Biotite	x	x	x	x	-	x	x	x	x	x	x	x	-	-	x	x
Hornblende	-	x	x	x	-	x	-	x	x	x	x	x	x	x	-	-
Garnet	x	x	x	x	x	x	x	x	x	-	-	-	-	-	-	-
Orthopyroxene	x	x	x	x	x	x	x	x	x	x	x	x	x	x	x	x
Clinopyroxene	x	x	x	x	x	x	x	x	x	x	x	x	x	x	x	x
Quartz	x	x	-	x	?	?	-	-	?	-	x	?	x	x	-	-
Paragenetic type	P3	P3	P3	P3	P3	P3	P3	P3	P3	P1	P1	P1	P1	P1	P1	P1

Table I (continued)

(d) Olivine Metagabbros

Sample No.	028	054	075	077	082-1	084	085-1	135
Biotite	x	x	x	x	x	x	x	x
Hornblende	-	x	x	x	x	x	x	x
Garnet	x	x	x	x	x	x	x	x
Orthopyroxene	x	x	x	x	x	x	x	x
Clinopyroxene	x	x	x	x	x	x	x	x

(- Quartz, + Plagioclase)

which is surrounded in turn by an inner shell of orthopyroxene and clinopyroxene, a thin layer of plagioclase and an outer shell of garnet - clinopyroxene simplectites. Plagioclase surrounding the garnet shell contains numerous tiny spinel inclusions.

In the case of an oxide core instead of olivine, the constituent minerals of the corona are different from those of a corona with an olivine core. The minerals surrounding the oxides are biotite or hornblende and garnet in successive shells. It is common to find the hornblende in contact with oxides without biotite and biotite in contact with oxides without hornblende.

Some samples have no spinel inclusions in plagioclase but tiny spinel inclusions in clinopyroxenes. Two possible hypotheses about the origin of spinel dusting in plagioclase have been advanced (Whitney, 1972; Whitney and McLelland, 1973). One is the trapping of spinel by plagioclase at a magmatic state and the other is the growth of spinel inclusions in plagioclase by sub-solidus reactions. Whitney (1972) preferred the second hypothesis through several observations, and described the possible reactions leading to the corona textures. The coronas between olivine and plagioclase are products of two reactions. The first reaction is the consumption of olivine and plagioclase and production of clinopyroxene, orthopyroxene and spinel. The second reaction consumes plagioclase, orthopyroxene, and spinel to produce garnet. The coronas surrounding oxides form by the reaction between oxides and plagioclase with the addition of magnesium. The second stage of these coronas is the formation of garnet (+ clinopyroxene) from hornblende (+ spinel). To have an addition of Mg from surroundings, the rock has to be an olivine - bearing one, because olivine reacts to form orthopyroxene producing Mg^{2+} and Fe^{2+} (Whitney & McLelland, 1983). In this type of corona, there may be a lot of biotite contacting oxides. But the role of biotite is not clear.

There are different opinions for the formation of coronitic textures. Coronas are generally believed to represent the metastable products of early subsolidus reactions

during cooling (Whitney, 1972; Whitney & McLelland, 1973, 1983; Grant, 1988). But Joesten (1986 a, b) presented textural evidence in favor of magmatic origin.

Whitney & McLelland (1983) claimed that coronitic textures surrounding olivine and oxides formed under granulite facies metamorphic conditions, either isobaric cooling or with increasing pressure at high temperature. However, the relation between the time of intrusion of gabbro and the time of peak metamorphism has never been clearly mentioned. Mineral assemblages found in the Olivine Metagabbro are shown in Table I (d). They belong to one type of assemblage.

2.2 Composition - paragenesis diagram

The mineral assemblages of the rocks in the Lake George Area are mostly of the hornblende-granulite facies in which both hydrous minerals and anhydrous minerals are stable. However, de Waard's subdivision of the granulite facies has not been successfully applied to the Lake George Area. Mineral assemblages of the rocks were classified into different paragenetic types in the previous section. An appropriate composition-paragenesis diagram has been sought. An ACF diagram is avoided here because it can not show the parageneses depending on the Fe/Mg ratio of the bulk-composition. Neither can the AFM diagram be used, because the CaO content is so high as to produce hornblende and clinopyroxene.

The CFM diagram of Abbott (1982) is tested to show the composition-paragenesis relations. The various mineral compositions are projected from quartz, H_2O, feldspar, and magnetite onto the C-F-M plane where $C = CaO + Na_2O + K_2O - Al_2O_3$, $F = FeO - Fe_2O_3$, $M = MgO$. Modal magnetite has been observed in most of the thin sections. The order of $X_{Fe} = Fe/(Fe+Mg)$ for coexisting CFM projected minerals is garnet > hornblende > biotite ≥ orthopyroxene > clinopyroxene. This order of X_{Fe} is

somewhat different from Abbott's. The partitioning of Fe and Mg between coexisting hornblende and orthopyroxene is reversed, X_{Fe} (Hnb) > X_{Fe} (Opx). And X_{Fe} of hornblende is higher than that of biotite. Abbott mentioned X_{Fe} of hornblende is higher than X_{Fe} of biotite in the condition of high pressure and low temperature, which is not the case in this study area.

There are 26 subfacies in Abbott's petrogenetic grid (Abbott, fig. 3, 1982). The mineral assemblages from the Lake George Area except these of the hornblende granitic gneisses, belong to subfacies 13 and 14 of Abbott's division. Most of the mineral assemblages of the Hornblende Granitic Gneisses belong to subfacies 8. Subfacies 8 is separated from subfacies 13 and 14 by different P, T conditions in the petrogenetic grid. The occurrence of Hornblende Granitic Gneiss, which is the major rock type in the study area, is not restricted to certain regions within this area. It is of random occurrence, being mixed with other rock types in the Lake George Area. Thus the P, T conditions of the Hornblende granitic gneiss cannot be different from the other lithologies. This inconsistency could be explained by a different CFM topology of the present study. Because of the difference in X_{Fe} between coexisting minerals, the CFM topology of the minerals from this study would differ from Abbott's.

Figure 2-3 a) shows the locations of the minerals from mainly mafic granulites and one charnockitic gneiss of the Lake George Area in the CFM diagrams. The compositions of minerals which are used in Fig. 2-3 are listed in Table II. Triangles in the figure 2-3 b, c indicate observed mineral assemblages from the study area. Two different CFM topologies of b) and c) can be drawn. The following tie-line exchange reaction can be written between Fig. 2-3 (b) and (c):

4 Biotite + 1 Hornblende + 29 Quartz = 23 Orthopyroxene + 1 Garnet + 8 K-feldspar + 1 Na-Plagioclase + 2 Ca-Plagioclase + 9 water

The occurrence of both mineral assemblages of CFM topology of (b) and (c) in Fig. 2-3 could be explained by variation in the activity of water.

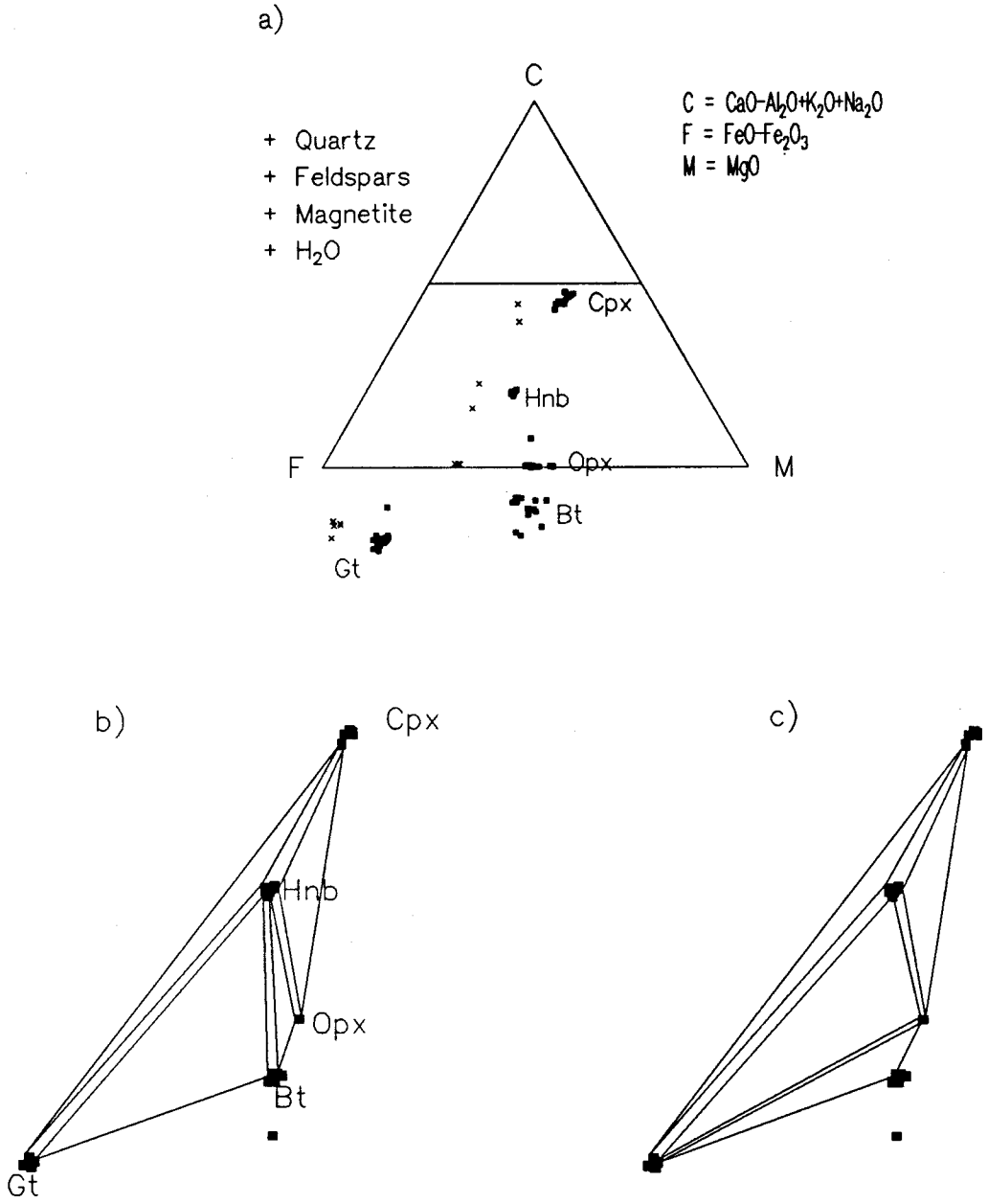

Fig. 2–3. a), Locations of minerals from the Lake George Area in the CFM diagram.
Filled squares, crosses are from the mafic granulites and the charnockitic gneisses, respectively.
b), c), Triangles were made for the observed mineral assemblages of the rocks.
Tie–line exchange reactiono occur between b) and c).
Cpx; clinopyroxene, Opx; orthopyroxene, Hnb; hornblende, Gt; garnet, Bt; biotite

Table II. Compositions of the minerals which are used in CFM diagram (in wt. %). Samples 03-1, 013 and 093 are mafic granulites. Sample 107 is from charnockitic gneiss. Nos. in the second column are the analyses nos. by microprobe.

Samp. No.	Mineral	SiO2	Al2O3	TiO2	FeO	MnO	MgO	CaO	K2O	Na2O
03-1a,18	Gt	38.760	21.550		28.420	1.370	4.000	7.270		
21	Gt	38.900	21.280		28.220	1.290	4.180	7.260		
24	Gt	38.620	21.410		28.010	1.320	4.160	7.300		
30	Gt	38.750	21.330		28.030	1.210	4.020	7.340		
66	Gt	38.550	20.950		27.810	1.370	4.070	7.260		
68	Gt	38.930	21.600		28.120	1.300	4.110	7.360		
69	Gt	38.720	21.310		28.270	1.360	4.130	7.250		
03-1a, 1	Opx	52.370	0.700	0.090	28.010	0.400	17.980	0.520		
2	Opx	52.230	0.740	0.070	27.460	0.380	18.180	0.530		
3	Opx	52.590	0.640	0.040	27.690	0.380	18.250	0.510		
81	Opx	51.530	0.830	0.060	29.070	0.400	16.810	0.550		0.010
82	Opx	51.700	0.800	0.030	29.330	0.400	16.650	0.520		0.000
43	Cpx	52.460	1.290	0.160	10.620	0.150	12.120	22.930		0.310
49	Cpx	52.900	1.390	0.170	11.750	0.180	11.890	22.690		0.360
51	Cpx	52.460	1.350	0.190	11.200	0.170	12.060	22.840		0.320
55	Cpx	52.080	1.460	0.170	11.440	0.220	11.640	22.400		0.330
56	Cpx	52.430	1.550	0.180	11.530	0.210	11.800	22.370		0.320
57	Cpx	51.760	1.420	0.210	12.340	0.270	11.720	21.990		0.320
79	Bt	36.890	14.680	5.680	18.140	0.020	10.130	0.460	8.720	0.100
80	Bt	35.080	14.380	5.320	17.730	0.000	10.890	0.100	8.960	0.090
03-1b,101	Gt	38.820	21.360		29.200	1.360	3.600	7.200		
104	Gt	38.830	21.230		28.870	1.340	3.640	7.360		
105	Gt	38.780	18.000		28.960	1.380	3.680	7.190		
121	Gt	38.810	21.320		28.950	1.320	3.710	7.220		
125	Gt	38.580	21.090		28.830	1.380	3.640	7.290		
140	Opx	51.780	0.580	0.020	30.520	0.470	16.240	0.480		0.010
145	Opx	51.350	0.590	0.060	30.550	0.410	16.110	0.490		0.020
146	Opx	51.660	0.610	0.060	30.640	0.450	16.070	0.580		0.010
149	Opx	51.590	0.650	0.060	30.660	0.480	16.280	0.560		0.020
152	Opx	51.300	0.650	0.050	30.920	0.510	15.950	0.550		0.020
153	Opx	51.440	0.630	0.050	30.400	0.450	15.940	0.570		0.010
150	Cpx	52.590	1.220	0.090	11.390	0.170	11.830	22.860		0.300
151	Cpx	52.440	1.340	0.120	11.630	0.180	11.710	23.050		0.310
134	Bt	35.110	5.760	5.460	18.430	0.050	9.830	0.300	8.720	0.100
136	Bt	35.130	15.180	5.620	18.480	0.020	10.240	0.200	8.680	0.090
137	Bt	35.390	15.270	5.850	18.450	0.050	10.010	0.160	8.800	0.080
138	Bt	35.270	15.420	5.400	18.440	0.040	9.940	0.220	8.920	0.100
03-1c,168	Gt	38.820	21.600		28.300	1.560	3.860	7.460		
169	Gt	38.760	21.900		28.700	1.570	3.890	7.100		
170	Gt	38.830	21.830		28.450	1.600	3.900	7.400		
172	Gt	38.640	21.820		28.580	1.550	4.120	7.230		
173	Gt	38.940	21.630		27.970	1.510	4.090	7.300		
157	Opx	51.370	0.760	0.060	29.870	0.540	15.990	0.590		
158	Opx	51.670	0.800	0.100	30.340	0.540	16.490	0.680		
159	Opx	51.280	0.810	0.030	30.200	0.580	16.510	0.570		
160	Cpx	51.950	1.790	0.240	11.810	0.260	11.420	23.330		0.380

Table II (continued)

Samp. No.	Mineral	SiO2	Al2O3	TiO2	FeO	MnO	MgO	CaO	K2O	Na2O
03-1c,161	Cpx	52.440	1.420	0.210	12.810	0.270	11.860	21.610		0.370
03-1d,175	Opx	51.530	0.840	0.050	30.250	0.530	16.100	0.540		0.010
178	Opx	51.770	0.620	0.080	30.270	0.500	16.100	0.510		0.010
179	Cpx	52.380	1.650	0.290	12.970	0.240	11.310	21.870		0.330
176	Bt	33.700	17.690	5.210	17.770	0.040	8.850	0.400	8.610	0.140
177	Bt	35.610	17.430	5.110	17.610	0.030	10.360	0.360	8.700	0.130
180	Bt	36.120	15.920	5.280	18.320	0.060	10.310	0.240	9.030	0.100
03-1e,183	Cpx	52.190	1.420	0.150	11.790	0.200	11.400	23.200		0.290
184	Cpx	52.520	1.350	0.150	11.570	0.210	11.380	23.190		0.310
185	Cpx	52.480	1.350	0.160	12.790	0.220	11.510	21.460		0.300
186	Opx	51.450	0.700	0.060	30.930	0.530	15.740	0.530		0.010
187	Opx	51.380	0.730	0.080	30.050	0.540	15.700	0.540		0.000
181	Bt	35.230	15.780	5.540	18.420	0.060	9.730	0.370	8.930	0.160
182	Bt	36.190	15.530	5.790	18.960	0.020	9.900	0.310	8.810	0.140
189	Bt	33.180	16.090	5.280	17.980	0.030	9.460	0.490	8.670	0.120
190	Bt	35.180	15.830	5.470	17.920	0.040	9.460	0.300	8.860	0.130
013a, 1	Gt	38.240	21.600		29.530	1.700	3.810	6.730		
2	Gt	38.120	21.470		29.340	1.740	4.020	6.620		
3	Gt	37.980	21.690		29.300	1.720	4.020	6.900		
6	Gt	38.070	21.500		29.390	1.510	4.090	6.780		
8	Gt	38.210	21.610		29.130	1.450	4.050	6.660		
9	Gt	37.870	21.520		29.820	1.520	3.950	6.850		
11	Opx	50.890	0.750		31.030	0.530	16.550	0.500		
13	Opx	50.950	0.700	0.120	31.010	0.520	16.680	0.430		
19	Cpx	51.130	1.810	0.160	13.170	0.230	11.100	21.340		0.440
20	Cpx	51.190	1.850	0.210	13.220	0.230	11.200	21.820		0.460
22	Cpx	51.060	1.900	0.270	14.320	0.250	11.140	20.700		0.450
23	Cpx	51.130	1.820	0.210	13.530	0.320	10.880	21.050		0.470
24	Cpx	51.420	1.950	0.150	13.080	0.290	11.190	21.360		0.470
14	Hn	41.070	12.090	2.240	19.250	0.140	8.400	11.220	1.860	1.370
15	Hn	40.730	12.400	2.260	19.350	0.170	8.370	11.010	1.790	1.280
27	Hn	41.260	12.110	2.120	19.020	0.020	8.500	11.390	1.900	1.360
28	Hn	41.090	12.390	1.860	19.270	0.070	8.410	11.310	1.920	1.160
17	Bt	36.140	14.150	5.650	20.380	0.010	10.080	0.030	9.040	0.070
18	Bt	36.100	14.240	5.280	20.960	0.020	10.040	0.020	9.270	0.010
013b, 52	Cpx	51.000	1.770	0.150	12.860	0.320	11.270	21.190		0.460
53	Cpx	51.680	1.740	0.110	12.830	0.300	11.420	21.420		0.450
58	Cpx	51.300	1.730	0.120	12.830	0.310	11.290	21.550		0.410
59	Cpx	51.290	1.710	0.040	12.660	0.310	11.250	21.380		0.420
60	Cpx	51.270	1.680	0.130	12.790	0.310	11.330	21.200		0.430
61	Cpx	51.300	1.760	0.130	12.790	0.330	11.210	21.060		0.440
38	Bt	35.290	14.690	5.380	20.800	0.040	9.550	0.140	8.900	0.090
39	Bt	35.370	14.520	5.300	20.900	0.060	9.860	0.130	8.920	0.080
40	Bt	36.070	14.350	5.310	21.010	0.060	10.020	0.030	9.230	0.020
41	Bt	36.010	14.340	5.490	21.090	0.050	9.920	0.040	9.230	0.040
42	Bt	35.800	14.800	5.480	20.850	0.080	9.960	0.050	9.160	0.040
44	Bt	34.680	17.470	5.470	19.500	0.040	9.290	0.250	8.420	0.120
46	Hn	41.210	12.320	1.960	19.570	0.170	8.380	11.370	1.870	1.410

Table II (continued)

Samp. No.	Mineral	SiO2	Al2O3	TiO2	FeO	MnO	MgO	CaO	K2O	Na2O
013b, 48	Hn	41.280	12.180	2.040	19.420	0.160	8.340	11.180	1.880	1.370
49	Hn	41.260	12.220	2.370	19.680	0.180	8.280	11.070	1.890	1.420
51	Hn	41.060	12.290	2.220	19.700	0.210	8.290	11.330	1.890	1.410
54	Hn	41.140	12.120	2.200	19.280	0.170	8.510	11.280	1.980	1.330
093-2a,71	Gt	38.290	21.790		29.920	0.910	3.990	6.800		
72	Gt	37.810	21.740		29.230	0.960	4.050	6.660		
73	Gt	38.220	21.690		29.220	0.870	4.020	6.910		
74	Gt	37.960	21.630		29.530	0.840	4.050	6.680		
75	Gt	37.890	21.780		29.410	0.910	4.050	6.840		
79	Cpx	51.280	1.610	0.180	11.650	0.170	12.050	21.520		0.440
80	Cpx	51.250	1.670	0.190	11.770	0.160	11.920	21.760		0.400
81	Cpx	51.910	1.380	0.170	11.540	0.170	12.010	21.930		0.390
82	Cpx	51.810	1.470	0.220	11.840	0.160	12.060	21.720		0.440
83	Opx	50.930	0.860	0.050	30.130	0.320	17.100	0.430		0.000
84	Opx	51.060	0.780	0.040	29.950	0.330	17.230	0.410		0.000
91	Hn	41.210	12.630	2.510	16.730	0.050	9.460	11.240	1.740	1.490
92	Hn	41.870	12.460	2.570	15.990	0.050	9.620	11.410	1.740	1.340
85	Bt	31.760	19.230	4.930	16.630	0.040	10.330	0.590	8.020	0.240
86	Bt	34.130	16.300	5.140	17.200	0.020	10.920	0.380	8.560	0.170
87	Bt	35.520	15.590	5.290	18.000	0.020	11.260	0.250	8.380	0.130
88	Bt	34.000	20.630	5.130	15.990	0.020	11.180	0.250	8.360	0.100
90	Bt	30.390	26.280	4.330	14.190	0.040	9.900	0.470	7.500	0.180
093-2b,110	Cpx	51.550	1.700	0.230	12.500	0.200	11.440	21.060		0.420
111	Cpx	51.390	1.750	0.250	12.850	0.230	11.470	21.140		0.400
112	Cpx	51.270	1.690	0.220	12.760	0.160	11.490	20.090		0.410
113	Cpx	51.480	1.700	0.180	12.360	0.190	11.560	21.330		0.400
114	Cpx	51.520	1.540	0.180	12.540	0.170	11.630	21.470		0.410
117	Op	50.580	0.870	0.070	31.520	0.430	16.270	0.400		0.000
101	Hn	41.150	12.790	2.380	17.160	0.110	9.150	11.000		1.440
102	Hn	40.980	13.050	1.980	17.600	0.090	9.340	11.270		1.400
107	Hn	40.720	12.860	2.540	17.490	0.100	8.800	11.150		1.600
108	Hn	41.080	13.020	2.150	17.070	0.120	9.120	11.210		1.460
109	Hn	41.000	12.850	2.100	17.240	0.100	9.030	11.270		1.480
093-2c,135	Gt	38.010	21.650		29.700	1.100	3.970	6.850		
136	Gt	37.970	21.680		29.740	1.000	3.950	6.880		
137	Gt	37.940	21.630		29.490	1.030	4.050	6.880		
138	Gt	37.950	21.690		30.130	1.050	3.930	6.830		
125	Cpx	51.280	1.280	0.150	11.260	0.150	12.280	21.530		0.360
126	Cpx	51.780	1.140	0.290	11.310	0.170	12.500	21.890		0.320
127	Cpx	51.450	1.480	0.130	11.560	0.150	12.120	21.370		0.350
128	Cpx	48.950	3.760	1.620	13.960	0.130	11.420	18.340		0.590
129	Cpx	50.080	2.910	0.640	12.600	0.130	11.600	19.890		0.500
132	Bt	29.730	25.860	4.640	15.320	0.030	8.940	0.460	7.540	0.300
133	Bt	35.530	14.930	5.550	18.950	0.050	10.790	0.170	9.070	0.060
145	Bt	30.020	25.370	4.660	15.320	0.030	8.900	0.450	7.750	0.300
120	Hn	40.270	12.960	2.470	17.100	0.040	8.910	11.150	1.710	1.540

Table II (continued)

Samp. No.	Mineral	SiO2	Al2O3	TiO2	FeO	MnO	MgO	CaO	K2O	Na2O
093-2c,121	Hn	41.190	12.610	2.470	17.160	0.050	9.210	11.050	1.710	1.570
122	Hn	40.680	12.530	2.330	17.280	0.070	9.140	11.160	1.740	1.460
123	Hn	41.010	12.740	2.150	17.090	0.040	9.260	10.950	1.700	1.420
124	Hn	40.940	12.950	2.190	17.400	0.050	9.190	10.960	1.670	1.480
093-2d,158	Cpx	51.600	1.530	0.130	12.030	0.200	11.690	21.650		0.380
159	Cpx	51.740	1.500	0.110	11.910	0.170	11.840	21.410		0.380
160	Cpx	51.420	1.530	0.110	12.150	0.170	11.630	21.480		0.400
161	Cpx	51.770	1.420	0.110	11.730	0.170	11.900	21.500		0.400
162	Cpx	51.630	1.450	0.100	11.630	0.150	12.040	21.900		0.360
153	Bt	36.080	14.840	5.240	17.440	0.000	12.490	0.120	9.180	0.140
154	Bt	36.380	14.670	5.260	17.180	0.020	12.600	0.090	9.220	0.090
156	Bt	35.600	14.900	5.600	18.880	0.030	10.950	0.120	9.090	0.090
146	Hn	40.890	12.970	2.240	17.150	0.060	8.960	10.970	1.690	1.520
147	Hn	40.850	13.050	2.500	17.420	0.080	9.160	11.200	1.730	1.590
148	Hn	41.170	12.960	2.160	17.060	0.040	9.160	11.460	1.700	1.430
149	Hn	40.930	12.860	2.600	17.230	0.080	9.090	11.450	1.680	1.520
150	Hn	41.010	12.660	2.680	17.110	0.090	9.090	11.390	1.730	1.400
152	Hn	40.980	12.880	2.500	17.390	0.060	9.030	11.230	1.700	1.530
107a,204	Gt	38.110	20.370		32.070	1.150	1.640	7.710		
211	Gt	38.110	20.550		32.090	1.140	1.650	7.840		
212	Gt	38.160	20.670		32.090	1.120	1.790	7.610		
201	Opx	49.160	0.560	0.110	39.070	0.380	9.870	0.650		
202	Opx	49.340	0.530	0.110	38.670	0.380	10.060	0.760		0.020
203	Opx	49.440	0.500	0.080	39.190	0.370	9.750	0.700		0.010
205	Opx	49.770	0.470	0.060	38.860	0.470	10.310	0.620		0.000
206	Hn	41.840	11.070	1.870	22.900	0.030	6.260	11.660	1.660	1.400
207	Hn	40.490	12.500	1.650	23.190	0.070	6.220	10.140	1.370	1.140
107b,216	Gt	37.880	20.620		30.660	1.260	1.980	7.740		
217	Gt	39.080	21.590		31.250	1.320	1.880	7.530		
223	Gt	37.900	20.440		30.890	1.180	1.940	7.700		
218	Cpx	48.430	9.570		16.000	0.170	7.010	19.350		0.540
219	Cpx	50.210	1.780		18.540	0.220	7.740	20.670		0.550

In figure 2-3 a), a different symbol is used for the minerals of the charnockitic gneisses. The charnockitic gneisses have higher FeO/MgO ratio than mafic granulites. Unfortunately, analyses of minerals of the hornblende granitic gneiss were not made. However I suspect that the FeO/MgO ratio may increase in the order: mafic granulites < charnockitic gneiss < hornblende granitic gneiss. If this is true, the absence of orthopyroxene in the hornblende granitic gneiss and presence of this mineral in charnocktic gneiss and mafic granulites may be largely due to the difference in the FeO/MgO ratio of the bulk-composition. Therefore, assemblages of the hornblende granitic gneisses do not necessarily belong to a different subfacies.

In Abbott's diagram, the CaO : Na_2O : K_2O ratio is not represented. The presence and amount of clinopyroxene, hornblende and biotite are largely controlled by this ratio, because clinopyroxene, hornblende and biotite contain CaO, Na_2O and K_2O respectively, as essential components. Furthurmore the ratio also influences the compositions of feldspars, which are ignored in Abbott's diagram.

2.3 Paragenesis of the biotite-garnet-sillimanite Gneiss

It is difficult to distinguish Biotite-garnet-sillimanite Gneiss from other quartzo-feldspathic gneisses because of almost same mineral assemblages. Only aluminous parts with biotite and garnet are described here. It is very common to have just sillimanite and garnet without biotite. Although kyanite has been reported to exist in a few places in the Adirondacks, sillimanite is the only aluminosilicate in the studied area. Primary muscovites have not been found, which indicates that the pressure and temperature condition of the metamorphism in the Lake George Area is beyond the muscovite decomposition curve in the petrogenetic grid. Sample 059-1 has been selected for detailed observation and microprobe analysis.

The peak metamorphic mineral assemblage in sample 059-1 is inferred to be garnet + biotite + sillimanite + quartz + K-feldspar + plagioclase + ilmenite + rutile. Retrograde alteration products of chlorites from garnet and biotites are also observed. There are four reactions that operate in this assemblage, ignoring any tschermak exchange reaction, in the SiO_2 - Al_2O_3 - FeO - MgO - MnO - CaO - Na_2O - K_2O - H_2O system:

$FeMg_{-1}$ (garnet) = $FeMg_{-1}$ (biotite) (1)

$FeMn_{-1}$ (garnet) = $FeMn_{-1}$ (biotite) (2)

$Al_2SiO_5 + KFe_3AlSi_3O_{10}(OH)_2 + 2\ SiO_2 = Fe_3Al_2Si_3O_{12} + KAlSi_3O_8 + H_2O$ (3)

$3\ CaAl_2Si_2O_8 = Ca_3Al_2Si_3O_{12} + 2\ Al_2SiO_5 + SiO_2$ (4)

Reactions 1, 2, and 3 proceed to the right with increasing temperature. Garnets in the sample 059-1 show chemical zoning. Figure 2-4 shows the element zoning profiles of garnets drawn in the box. Three profiles represent different cross sections of garnets, A-A', B-B' and C-C', respectively. Cross sections A-A' and B-B' are in the garnet 1 which is surrounded by biotites and C-C' is in the garnet 2 which is not in contact with biotite. Almandine content tends to increase toward the rim whereas pyrope content decreases. Grossular has a rather irregular pattern, but commonly shows a slight increase near the rim. It is difficult to conclude anything about spessartine because it does not show a regular trend. Profiles of Fig. 2-4 a) and b) show a more distinctive change than c), which has a rather flat profile. Garnet 1 was more deeply involved in reactions than garnet 2. The zoning pattern of almandine content can be caused by the operation to the left of the reactions 1 and 3 with decreasing temperature. The broad flat pattern in the middle of the both garnets may be ascribed to diffusion at high temperature. An AFM 3-phase triangle garnet-biotite-sillimanite is drawn in Fig. 2-5. The triangle with solid lines is from the compositions in the core of garnet and biotites in the matrix. The one with broken lines is from the compositions of the rim of the garnet and biotite contacting the garnet. The triangle moved to more Fe-rich compositions. The change of

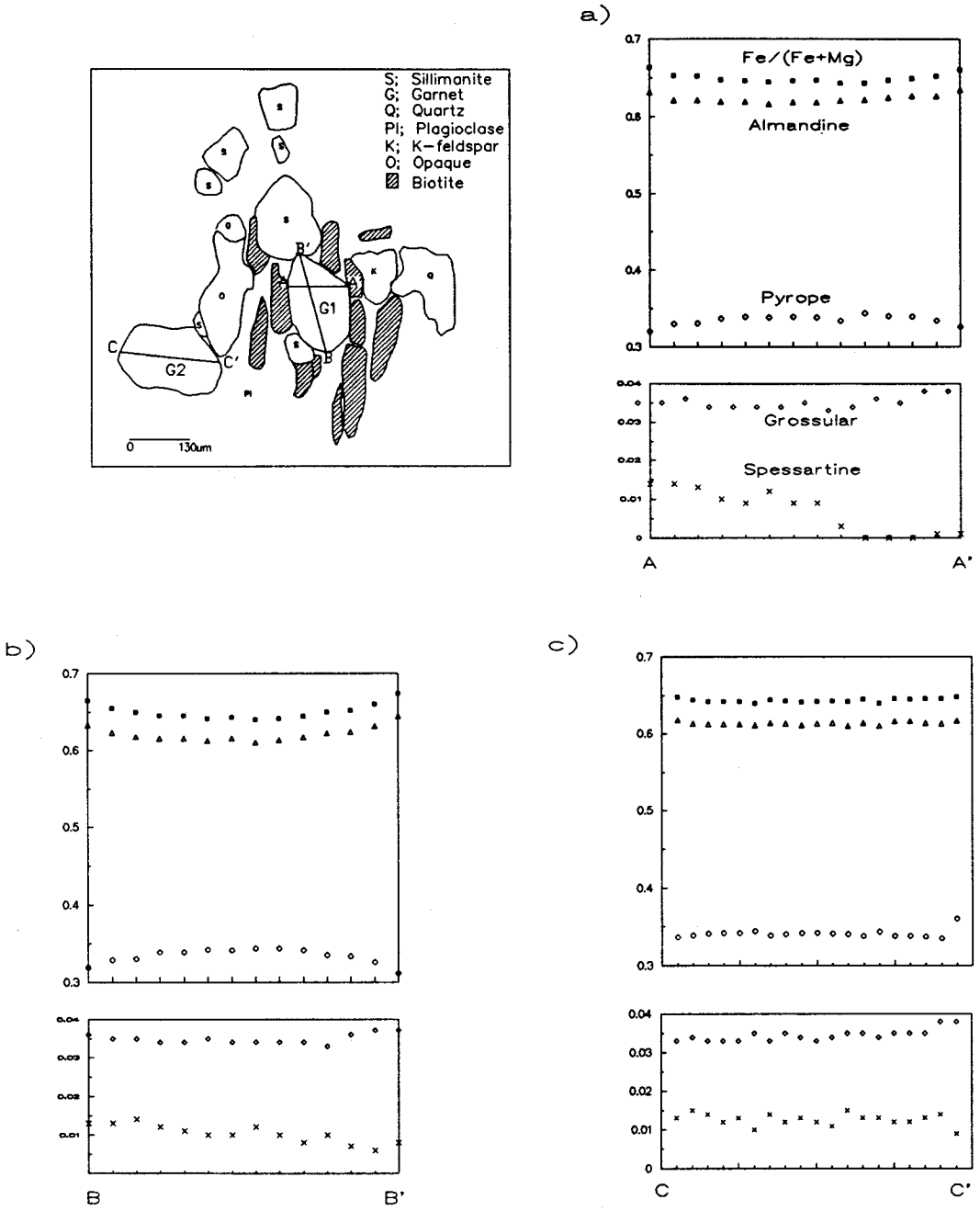

Fig. 2-4. Zoning profiles of garnets from sample 059-1. a), b) and c) show different sections of garnets. A-A', B-B' and C-C' are drawn in the box at the upper left.

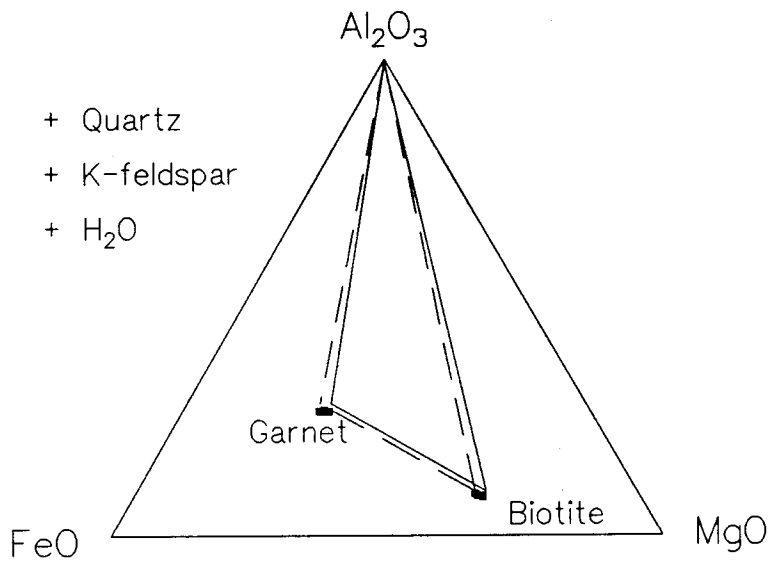

Fig. 2-5. AFM diagram of the biotite-garnet-sillimanite gneiss. Positions of the minerals are from sample 059-1. Solid line is from compositions of core of garnet and biotite in the matrix, broken line is from compositions of rim of garnet and biotite contacting garnet.

position of the triangle to the left means net transfer reaction (3) dominated exchange reaction (1). Zonation was observed also in the plagioclase. Anorthite component increases toward rim. It can be inferred that rock also experienced reaction (4).

The problem remains whether the composition of the core of garnet is that of the peak metamorphism. At high temperature, diffusivity of Fe and Mg in the garnet is high enough to erase the composition at the peak metamorphism especially with slow cooling. It is, therefore, difficult to get the compositions of minerals at the peak metamorphism.

2.4 Biotite

It is known that the color of biotite changes with metamorphic grade and the color is directly related to Ti content of the biotite. But, it is necessary to know what are the Ti-minerals in the rock. Otherwise, the Ti-content of biotite vary with the bulk-rock composition. For example, the Ti-free rocks produce only Ti-free biotite, whatever the metamorphic grade is. In other studies, biotites are associated with ilmenite (Schreurs, 1985) and ilmenite±rutile (Dymek, 1983). Biotites in the Lake George Area always coexist with ilmenite which, commonly with accompanying rutile or sphene. Biotites of brown or reddish brown color were observed in this region, which indicates high grade metamorphism. Biotites coexist with garnet, clinopyroxene, orthopyroxene and hornblende in metamorphosed igneous rocks and mainly with garnet in metapelites. The Ti content of most of the biotites varies between 5 wt% to 6 wt%. The compositions of biotites are given in Table III. The compositional variation with metamorphic grade has been studied (Schreurs, 1985), and the Ti content was found to increase with decreasing Al^{VI} content. Schreurs suggested the numerical values for certain metamorphic facies. Ti > 0.45 and Al^{VI} < 0.55 atoms/formula unit (based on 22

Table III. Element proportions of biotites from the Lake George Area (based on 11 Oxygens). a), Biotites from mafic granulites. b), Biotites from metapelites.

a)

Sample No	Si	Al(IV)	Al(VI)	Ti	Mg	Fe	Mn	Ca	Na	K
03-1a, 80	2.7451	1.2549	0.0713	0.3131	1.2710	1.1601	0.0010	0.0084	0.0134	0.8948
79	2.8043	1.1957	0.1193	0.3245	1.1479	1.1531	0.0014	0.0373	0.0141	0.8454
1b,134	2.7007	1.2993	0.0842	0.3396	1.1901	1.2004	0.0026	0.0164	0.0102	0.8583
137	2.7251	1.2749	0.1112	0.3389	1.1495	1.1878	0.0031	0.0133	0.0123	0.8648
1d,177	2.6839	1.3161	0.2315	0.2893	1.1633	1.1097	0.0018	0.0289	0.0196	0.8363
1e,180	2.7368	1.2632	0.1586	0.3009	1.1642	1.1609	0.0036	0.0195	0.0141	0.8724
182	2.7404	1.2596	0.1260	0.3299	1.1181	1.2004	0.0015	0.0251	0.0200	0.8506
190	2.7291	1.2709	0.1765	0.3190	1.0939	1.1627	0.0028	0.0249	0.0190	0.8768
013a, 17	2.7654	1.2346	0.0422	0.3254	1.1504	1.3043	0.0008	0.0025	0.0099	0.8820
18	2.7618	1.2382	0.0453	0.3040	1.1452	1.3411	0.0011	0.0019	0.0018	0.9047
40	2.7551	1.2449	0.0468	0.3053	1.1410	1.3421	0.0040	0.0028	0.0033	0.8992
41	2.7494	1.2506	0.0397	0.3151	1.1295	1.3467	0.0033	0.0029	0.0056	0.8990
42	2.7537	1.2463	0.0297	0.3167	1.1417	1.3410	0.0050	0.0043	0.0056	0.8987
43	2.6646	1.3354	0.1179	0.3226	1.1230	1.2837	0.0025	0.0189	0.0169	0.8171
44	2.6415	1.3585	0.2277	0.3131	1.0544	1.2423	0.0027	0.0205	0.0182	0.8179
93-2a, 85	2.4907	1.5093	0.2683	0.2905	1.2080	1.0907	0.0024	0.0500	0.0365	0.8026
86	2.6528	1.3472	0.1463	0.3005	1.2650	1.1178	0.0011	0.0318	0.0251	0.8488
87	2.7103	1.2897	0.1120	0.3035	1.2812	1.1488	0.0014	0.0204	0.0196	0.8156
88	2.5281	1.4719	0.3354	0.2870	1.2393	0.9940	0.0014	0.0202	0.0145	0.7926
89	2.4034	1.5966	0.4786	0.2873	1.0795	0.9985	0.0020	0.0225	0.0175	0.7882
90	2.2917	1.7083	0.6268	0.2453	1.1126	0.8948	0.0026	0.0384	0.0270	0.7217
93-2c,131	2.2726	1.7274	0.6021	0.2667	1.0192	0.9789	0.0018	0.0377	0.0438	0.7347
132	2.7180	1.2820	0.0636	0.3190	1.2306	1.2121	0.0035	0.0143	0.0087	0.8847
133	2.4216	1.5784	0.4574	0.2729	1.1059	1.0226	0.0027	0.0493	0.0411	0.7116
93-2d,153	2.7257	1.2743	0.0473	0.2975	1.4070	1.1017	0.0000	0.0095	0.0212	0.8843
154	2.7439	1.2561	0.0483	0.2981	1.4164	1.0838	0.0013	0.0073	0.0136	0.8866
156	2.7174	1.2826	0.0580	0.3213	1.2459	1.2047	0.0021	0.0096	0.0128	0.8847

b)

	Si	Al(IV)	Al(VI)	Ti	Mg	Fe	Mn	Ca	Na	K
59-1a,2	2.7508	1.2492	0.1370	0.2740	1.6556	0.7567	0.0017	0.0009	0.0053	0.9065
2	2.7396	1.2604	0.1175	0.2773	1.6451	0.7917	0.0000	0.0006	0.0030	0.9197
2	2.7493	1.2507	0.1133	0.2787	1.6546	0.7794	0.0006	0.0008	0.0042	0.9200
2	2.7224	1.2776	0.1038	0.2840	1.6559	0.7963	0.0000	0.0020	0.0056	0.9151
2	2.7444	1.2556	0.1164	0.2807	1.6686	0.7491	0.0000	0.0033	0.0091	0.9320
2	2.7508	1.2492	0.1189	0.2811	1.6300	0.7889	0.0000	0.0026	0.0105	0.9135
2	2.7360	1.2640	0.1130	0.2863	1.1423	0.7852	0.0000	0.0021	0.0045	0.9153
2	2.7593	1.2407	0.1510	0.2722	1.6225	0.7550	0.0027	0.0021	0.0089	0.9246
2	2.7262	1.2738	0.1207	0.2776	1.6437	0.7738	0.0018	0.0000	0.0060	0.9557
3	2.7302	1.2698	0.1194	0.2905	1.6069	0.7981	0.0050	0.0000	0.0073	0.9211
3	2.7477	1.2523	0.1353	0.2661	1.6536	0.7675	0.0065	0.0000	0.0051	0.9218
3	2.7263	1.2737	0.1303	0.2691	1.6659	0.7785	0.0077	0.0000	0.0082	0.8931
3	2.7338	1.2662	0.1024	0.2800	1.6879	0.7497	0.0105	0.0000	0.0100	0.9319
3	2.7230	1.2770	0.1099	0.2763	1.6691	0.7705	0.0126	0.0011	0.0102	0.9245

oxygens) indicates low to intermediate-granulite facies. Those values from the study area belong to the granulite facies. Also, study has been made of the correlation of the composition of biotites to the metamorphic temperature in the Northwest Adirondacks (, 1989). According to this latter study, the composition of biotites in rocks of the Lake George Area indicates a metamorphic temperature of near 700°C.

An appropriate composition diagram of the biotites from the Lake George Area is illustrated in Fig. 2-6. Most biotites fall in the compositional field close to the middle of eastonite-siderophyllite series. Biotites from the metapelite are closer to eastonite. Those in metabasite show much more variation in Al-content. The substitution mechanisms for the biotites of high grade rocks has been suggested (Dymek, 1983; Schreurs, 1985). The relationships of Ti - Al^{VI} content and Al^{IV} - Al^{IV} content of the biotites are illustrated in Fig. 2-7. High Ti-content in the granulite is explained by Ti-Tschermak substitution:

$$(R^{2+})^{VI} + 2\,(Si^{4+})^{IV} = (Ti^{4+})^{VI} + 2\,(Al^{3+})^{IV} \qquad (5)$$

Many biotites from the Lake George Area fall above the line in Fig. 2-7 (a), indicating additional Ti substitution mechanisms. Al-enrichment in biotites of the granulite facies has been explained mainly by Al-Tschermak's substitution:

$$(R^{2+})^{VI} + (Si^{4+})^{IV} = (Al^{3+})^{VI} + (Al^{3+})^{IV} \qquad (6)$$

If the substitution of Al^{VI} occurred only by (6), the points should lie along the line in Fig. 2-7 b. The biotites from the present study fall below the line suggesting the presence of other substitution mechanisms for the VI-fold site of biotites. This plot of elements in biotites from the Lake George Area differs from the data of other biotites of the granulite facies (Dymek, 1983). In Dymek's study, biotites of metapelitic gneisses lie below the line of $Ti/(Al^{IV}-1) = 1/2$ in Fig. 2-7 a, and above the line of $(Al^{IV}-Al^{VI}) = 1$ in Fig. 2-7 b. It seems that substitution mechanisms may also be controlled by other factors. Mineral analyses in this study were done by microprobe analysis techniques and

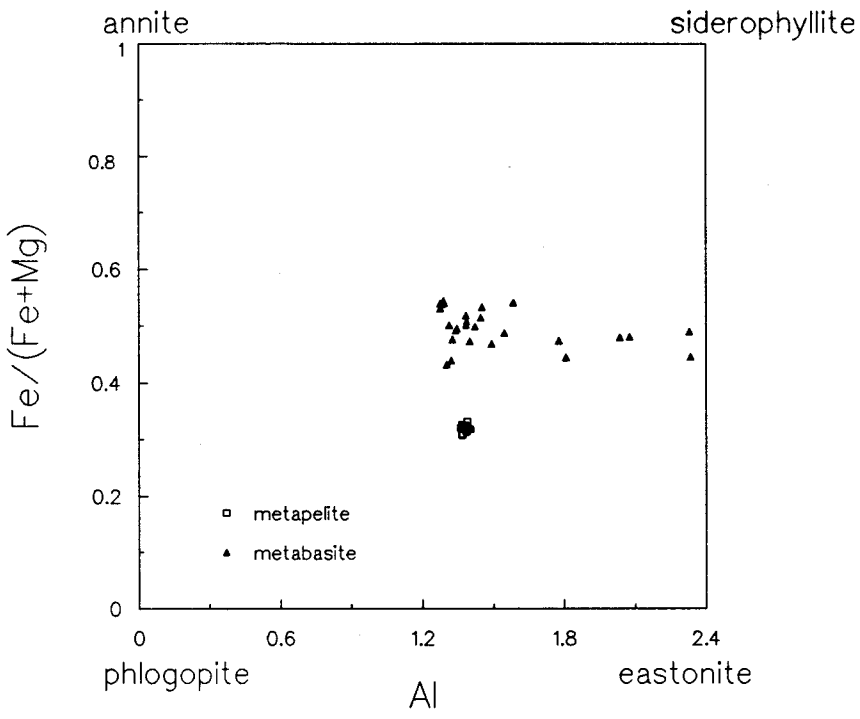

Fig. 2-6. Compositional field of biotites of metapelites and metamorphosed igneous rocks in the Lake George Area.

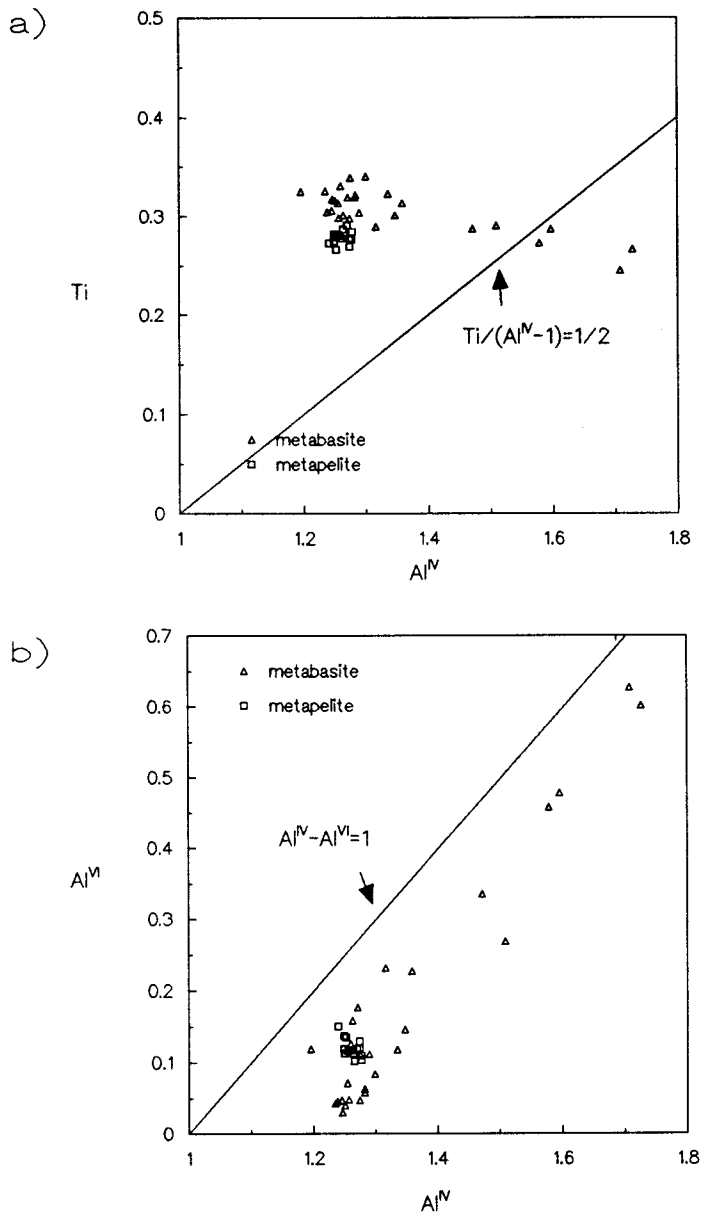

Fig. 2-7. a). Ti and Al^{IV} contents of biotites from the Lake George Area.

b). Relationships of Al^{VI} and Al^{IV} in biotites from the Lake George Area.

Fe^{3+} and other volatile component could not be determined. Additional detailed analysis is needed to infer other substitution mechanisms.

CHAPTER 3. P-T CONDITION OF THE METAMORPHISM

3.1 Introduction.

The estimation of temperature and pressure at the peak-metamorphic conditions has been one of the main subject of studies in metamorphic petrology. Knowledge of the pressure and temperature conditions which have been experienced by rocks give a better understanding of the tectonic history of the rocks. With the development of experimental apparatus and more reliable and abundant experimental thermodynamic data, it has become possible to get better constrained results. Especially with the aid of a computer, it has become quite straightforward to do such a study, even though the interpretation of results is far from simple.

It is well known that rocks of the Adirondack Highlands belong to the granulite facies. Metamorphic temperatures in the Adirondacks have been estimated by a number of investigators with different techniques. Temperatures of 550°C ± 50°C near the Lowlands-Highlands boundary, and 650°C ± 50°C in the central Adirondacks (Engel & Engel, 1958) now appear to be too low. De Waard (1967b) estimated metamorphic temperatures of 675 - 700°C near the boundary between the High-Low Lands, and about 800°C near the central Adirondacks. These temperature estimates are consistent with those made later by Bohlen and Essene (1977, 1985). From the synthesis of other studies of metamorphic temperatures, Bohlen et al. (1985) confirmed results of their earlier study based on feldspar and iron-oxide geothermometry (Bohlen and Essene, 1977). The results were depicted as a series of concentric isotherms in the Adirondack Highlands. It appears that the majority of geologists accepted their isotherm pattern.

Metamorphic pressures have also been estimated by Bohlen et al. (1985). Based on their metamorphic temperatures combined with geobarometric studies, they inferred a concentric pattern for pressure distribution. In other words, they also concluded that

metamorphic pressure increases toward the center of the Adirondack Highlands from the margin. The Lake George Area lies at the southeastern tip of the Adirondack Highlands. I want to investigate whether the metamorphic temperatures and pressures in this area will fit into the temperature and pressure patterns of the Adirondack Highlands that were suggested by Bohlen at al. (1985). There is an estimate of P-T condition by liquidus equilibria of granitic pegmatites in the present study area (Putman & Sullivan, 1979). They gave about 7kb and 660-690°C. Furthermore, I would like to discuss the problems involved in the estimation of the P-T conditions of the metamorphism.

3.2 Methodology.

Mineral analyses were obtained using a JOEL Superprobe 733 with wavelength dispersive PET, LIF and TAP crystal spectrometers. An Acceleration potential of 15 KeV and a beam current of 17 - 21 nA were operating conditions, with counting times of 11 - 40 seconds. Beam sizes were less than 10 μm. Analyses were reduced using the corrections of Bence and Albee (1968). In order to observe inclusions or other textures inside minerals, back-scattered electron images were used. Compositional variations within the minerals of interest were checked. Garnet, pyroxene, amphibole, biotite, feldspar and iron-oxides were normalized to 12, 6, 23, 11, 8 and 3 oxygens, respectively. Fe in the table (Table IV, V, VI) means total iron.

I tried to find mineral assemblages which are suitable for geothermobarometry. It was not easy to find good assemblages because of heavy alteration and many inclusions. In petrographic examination, sample Ar003-1 belonging to the mafic granulites was found to be comparatively good. This sample contains garnet, pyroxenes, plagioclse and quartz and can thus be used for garnet-pyroxenes thermometers and garnet-plagioclase-pyroxenes-quartz barometers.

In a P-T diagram, the solid-solid exchange reaction has a steep slope so that it is sensitive to the change in temperature, whereas the net-transfer reaction has a shallow slope so that it is sensitive to the variation in pressure. From the intersections of these two sets of curves on the P-T diagram, the P-T condition of equilibrium can be estimated graphically. Three parts of one thin-section of sample Ar003-1 have been investigated to have better estimation.

3.3 Calibrations Used.

Because of the common mineral assemblage in mafic granulites of garnet + pyroxenes, accompanied by plagioclase and quartz, garnet-orthopyroxene(clinopyroxene) thermometers and garnet-plagioclase-orthopyroxene(clinopyroxene)-quartz barometers were chosen. Basic ion-exchange and net-transfer reactions applicable to this assemblage are as follows;

Garnet-orthopyroxene exchange reaction.

$$3\ MgSiO_3 + Fe_3Al_2Si_3O_{12} = 3\ FeSiO_3 + Mg_3Al_2Si_3O_{12}$$

Garnet-clinopyroxene exchange reaction.

$$1/3\ Mg_3Al_2Si_3O_{12} + CaFeSi_2O_6 = 1/3\ Fe_3Al_2Si_3O_{12} + CaMgSi_2O_6$$

Garnet-plagioclase-orthopyroxene-quartz net-transfer reaction.

$$CaAl_2Si_2O_8 + Mg_2Si_2O_6 = 1/3\ Ca_3Al_2Si_3O_{12} + 2/3\ Mg_3Al_2Si_3O_{12} + SiO_2$$

Garnet-plagioclse-clinopyroxene-quartz net-transfer reaction.

$$CaAl_2Si_2O_8 + CaMgSi_2O_6 = 2/3\ Ca_3Al_2Si_3O_{12} + 1/3\ Mg_3Al_2Si_3O_{12} + SiO_2$$

Several calibrations of these reactions, which are believed to be useful in the determination of the P-T conditions of the granulite facies, are shown in Fig. 3-2. For details of each calibration, the reader is referred to the relevant papers cited. Since

different thermodynamic data and different activity parameters were used in these calibrations, some variation in results is to be expected as shown in Fig. 3-2.

3.4 Results

3.4.1 Sample Ar003-1a

Mineral relations of the mafic granulite sample Ar003-1a are schematically shown in the sketch of Fig. 3-1. A grain of garnet which has a small orthopyroxene as an inclusion occurs in the lower middle of the sketch. Two other garnets are in contact with clinopyroxenes. For the garnet-orthopyroxene thermobarometry, the garnet with the orthopyroxene inclusion and the orthopyroxene inclusion itself were used. Garnet and clinopyroxene in direct contact shown at the right of the sketch were used for a garnet-clinopyroxene thermometer and barometer. Representative mineral compositions are listed in Table IV. Slight variations in compositions were observed in some minerals. The Fe/Mg ratio in garnets increases toward the orthopyroxene inclusion and the contact with clinopyroxenes. Clinopyroxenes also show some compositional variation near the rim.

The diagrams of Fig. 3-2 gives P-T conditions retrieved from the garnet-orthopyroxene thermobarometry (Fig. 3-2, (a)) and garnet-clinopyroxene thermobarometry (Fig. 3-2, (b)). A stability field of aluminosilicates (Holdaway, 1971) are also shown for a reference and limitations. The numbers in both P-T diagrams are the corresponding calibrations. Every calibration yields two slopes because of variations of compositions. The left or lower slopes are obtained from the compositions of the two minerals at the contact and the right or upper slopes are from the compositions of the cores of the same minerals but not at the contact with each other. Different calibrations give different estimates of P-T conditions. Harley's garnet-orthopyroxene thermometer

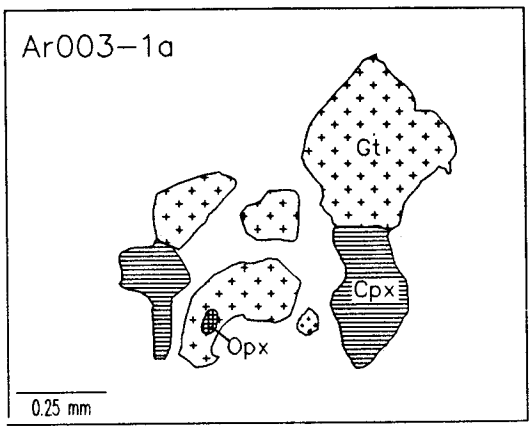

Fig. 3-1. A schematic sketch of sample Ar003-1a.

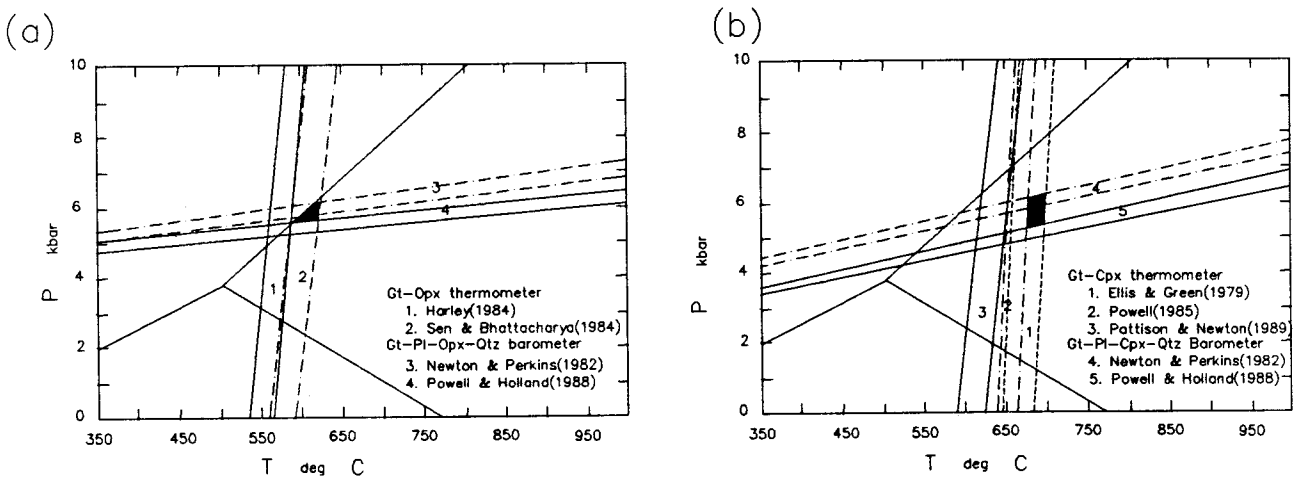

Fig. 3-2. P-T diagrams showing pressure-temperature conditions for sample Ar003-1a, using garnet-orthopyroxene, garnet-plagioclase-orthopyroxene-quartz thermobarometers (a), and garnet-clinopyroxene, garnet-plagioclase-clinopyroxene-quartz thermobarometers (b). The filled boxes are made with the highest values of P-T condition of each calibration. Calibration 3 in diagram (b) is not used.

Table IV. The compositions of the minerals of sample Ar003-1a.

	Garnet						Orthopyroxene				Plagioclase	
	core			rim			core		rim			
SiO2	38.80	38.76	38.62	38.73	38.62	38.75	52.23	52.29	52.37	52.33	58.58	57.94
Al2O3	21.57	21.55	21.32	21.45	21.41	21.50	0.74	0.64	0.70	0.56	27.40	27.31
TiO2							0.07	0.04	0.09	0.07		
FeO	28.23	28.42	28.01	28.02	28.01	28.09	27.46	27.69	28.01	27.91	0.06	0.05
MnO	1.31	1.37	1.35	1.35	1.32	1.34	0.38	0.38	0.40	0.40		
MgO	3.87	4.00	3.97	3.99	4.16	4.10	18.18	18.25	17.98	17.96		
CaO	7.38	7.27	7.39	7.30	7.30	7.24	0.53	0.51	0.52	0.48	9.14	9.12
Na2O												
K2O												
ToTal	101.16	101.37	100.67	100.83	100.83	101.02	99.61	100.10	100.06	99.70	101.52	100.73
Si	3.0209	3.0146	3.0222	3.0231	3.0161	3.0196	1.9980	2.0020	1.9985	2.0037	2.5816	2.5746
Al	1.9791	1.9749	1.9666	1.9735	1.9707	1.9741	0.0333	0.0289	0.0314	0.0250	1.4231	1.4301
Ti							0.0021	0.0011	0.0025	0.0019		
Fe	1.8300	1.8483	1.8332	1.8289	1.8292	1.8298	0.8785	0.8815	0.8938	0.8935	0.0022	0.0017
Mn	0.0866	0.0900	0.0893	0.0890	0.0873	0.0887	0.0124	0.0123	0.0129	0.0129		
Mg	0.4495	0.4639	0.4633	0.4646	0.4843	0.4765	1.0369	1.0355	1.0227	1.0249		
Ca	0.6153	0.6059	0.6194	0.6106	0.6109	0.6043	0.0218	0.0209	0.0213	0.0199	0.4313	0.4340
Na											0.5288	0.5303
K											0.0082	0.0092
Total	7.9890	7.9975	7.9939	7.9897	7.9980	7.9929	3.9831	3.9822	3.9830	3.9816	4.9751	4.9798

	Garnet			Clinopyroxene			
SiO2	38.54	38.67	38.63	52.08	52.46	52.83	52.47
Al2O3	21.18	21.25	21.34	1.46	1.37	1.25	1.22
TiO2				0.17	0.17	0.14	0.14
FeO	28.21	27.93	28.05	11.44	11.39	10.26	10.54
MnO	1.28	1.32	1.34	0.22	0.27	0.23	0.20
MgO	4.12	4.09	4.07	11.64	11.83	12.19	12.41
CaO	7.18	7.17	7.28	22.40	22.37	23.52	23.20
Na2O				0.33	0.33	0.29	0.31
K2O							
ToTal	100.52	100.44	100.71	99.73	100.21	100.69	100.49
Si	3.0222	3.0298	3.0211	1.9723	1.9758	1.9749	1.9683
Al	1.9573	1.9624	1.9665	0.0653	0.0610	0.0549	0.0538
Ti				0.0050	0.0049	0.0039	0.0040
Fe	1.8439	1.8298	1.8346	0.3622	0.3588	0.3027	0.3306
Mn				0.0070	0.0086	0.0072	0.0064
Mg	0.4818	0.4771	0.4742	0.6570	0.6645	0.6796	0.6940
Ca	0.6034	0.6018	0.6099	0.9089	0.9028	0.9418	0.9322
Na				0.0241	0.0243	0.0210	0.0223
K							
Total	7.9887	7.9885	7.9951	4.0018	4.0007	4.0040	4.0116

(1984) gives a lower temperature than Sen & Bhattacharya's by about 30 to 40 degrees in Centigrade. Pressures obtained with calibration by Powell and Holland (1988) give a lower value than with Newton and Perkins (1982) by 0.5 kbar. With experiments of Fe-end member garnet-plagioclase-orthopyroxene-quartz reaction at the P-T condition of the granulite facies, Bohlen et al. (1983) presented garnet-plagioclase-orthopyroxene-quartz barometer. They claimed that their barometer works well in most of the granulite facies except the case of resetting of the compositions of the phases during retrograde metamorphism. Bohlen's calibration turned out to give higher value than others by 2 kbars, which is in the kyanite stability field. Therefore I did not use his calibration. Taking four calibrations from the use of compositions of cores of minerals, The area of intersection was found for the garnet-orthopyroxene thermobarometry within the stability field of sillimanite in (a) of fig. 3-2 (filled area). Values of 630°C, 6.2 kbar, and 590°C, 5.5 kbar were obtained for the highest and lowest P-T conditions, respectively, for sample Ar003-1a.

Estimates of P-T conditions obtained from garnet-clinopyroxene equilibrium for the same sample (Ar003-1a) is shown in Fig. 3-2 (b). With compositions of cores of the minerals, values of 680 - 700°C, 5.3 - 6.3 kbar were inferred from four calibrations. For comparison, a calculation by Pattison & Newton (1989) is represented by number 3. It gives 650 - 660°C, 5.2 - 6.0 kbar as a P-T condition by intersection with the two barometers (#4,5) for the same compositions.

3.4.2 Sample Ar003-1b

A sketch of the mineral assemblages which were used for the garnet-clinopyroxene(orthopyroxene) thermometers and garnet-plagioclase-clinopyroxene(orthopyroxene)-quartz barometers is shown in Fig. 3-3 (a). A large grain of garnet is surrounded by rather small grains of orthopyroxene, biotite, ilmenite,

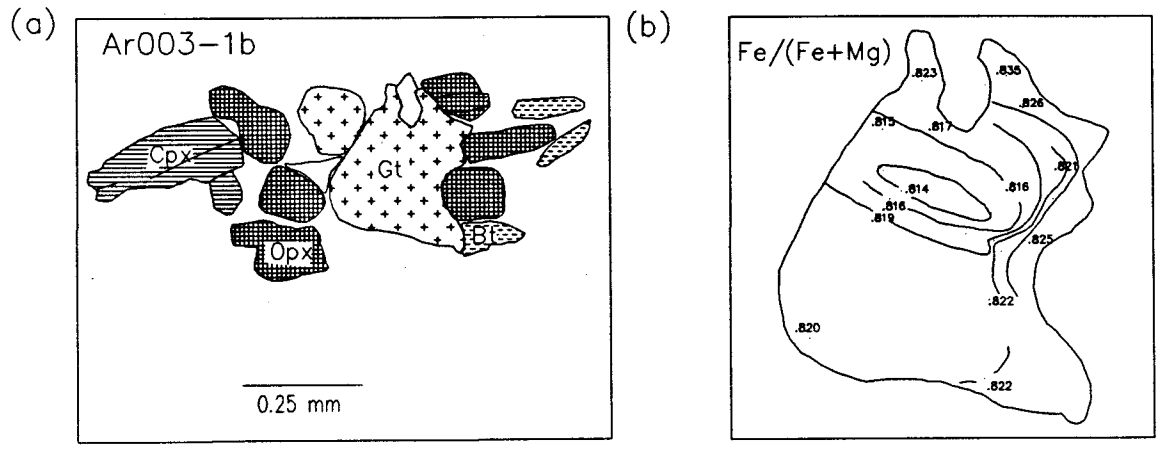

Fig. 3-3. (a). A schematic sketch of sample Ar003-1b.
(b). A compositional map of a garnet in the middle of Fig. 3-3 (a).

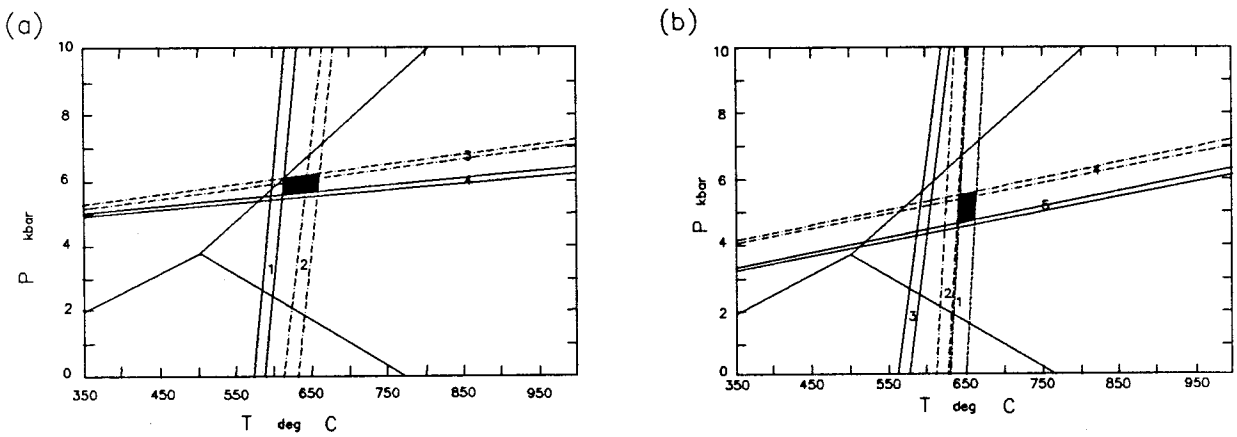

Fig. 3-4. P-T diagrams showing P-T conditions for sample Ar003-1b, estimated with garnet-orthopyroxene, garnet-plagioclase-orthopyroxene-quartz thermobarometers(a), and garnet-clinopyroxene, garnet-plagioclase-clinopyroxene-quartz thermobarometer(b). Numbers in the boxes are referred to Fig. 3-2.

Table V. The compositions of the minerals of sample Ar003-1b.

	Garnet							Orthopyroxene					
	core				rim			matrix		core		rim	
SiO2	38.79	38.83	38.51	38.58	38.51	38.71	38.90	51.30	51.44	51.66	51.43	51.78	51.81
Al2O3	21.50	21.23	21.17	21.09	21.44	21.48	21.28	0.65	0.63	0.61	0.52	0.58	0.74
TiO2								0.05	0.05	0.06	0.04	0.02	0.07
FeO	28.98	28.87	28.77	28.83	29.44	29.20	29.18	30.92	30.40	30.64	30.28	30.52	30.59
MnO	1.32	1.34	1.39	1.38	1.36	1.40	1.37	0.51	0.45	0.45	0.45	0.47	0.44
MgO	3.58	3.64	3.63	3.64	3.48	3.51	3.47	15.95	15.94	16.07	16.16	16.24	16.23
CaO	7.16	7.36	7.32	7.29	7.27	7.19	7.26	0.55	0.57	0.58	0.63	0.48	0.56
Na2O								0.02	0.01	0.01	0.03	0.01	0.01
K2O													
Total	101.33	101.27	100.79	100.81	101.50	101.49	101.45	99.95	99.50	100.07	99.53	100.09	100.44
Si	3.0237	3.0299	3.0216	3.0265	3.0074	3.0175	3.0324	1.9922	2.0006	1.9988	1.9994	2.0011	1.9956
Al	1.9753	1.9525	1.9576	1.9498	1.9730	1.9732	1.9554	0.0298	0.0289	0.0278	0.0237	0.0264	0.0334
Ti								0.0014	0.0015	0.0016	0.0012	0.0005	0.0020
Fe	1.8887	1.8835	1.8877	1.8913	1.9221	1.9037	1.9019	1.0040	0.9887	0.9912	0.9845	0.9861	0.9851
Mn	0.0875	0.0887	0.0921	0.0917	0.0901	0.0927	0.0902	0.0169	0.0148	0.0148	0.0148	0.0153	0.0142
Mg	0.4155	0.4238	0.4247	0.4257	0.4048	0.4079	0.4032	0.9236	0.9243	0.9269	0.9366	0.9356	0.9317
Ca	0.5976	0.6151	0.6153	0.6131	0.6084	0.6004	0.6062	0.0228	0.0238	0.0240	0.0262	0.0197	0.0232
Na								0.0012	0.0011	0.0007	0.0020	0.0008	0.0007
K													
Total	7.9881	7.9933	7.9991	7.9981	8.0056	7.9954	7.9893	3.9918	3.9837	3.9858	3.9883	3.9854	3.9858

	Clinopyroxene		Plagioclase		
SiO2	52.59	52.44	57.98	57.82	58.09
Al2O3	1.22	1.34	27.44	27.22	27.32
TiO2	0.09	0.12			
FeO	11.39	11.63	0.20	0.19	0.13
MnO	0.17	0.18			
MgO	11.83	11.71			
CaO	22.86	23.05	9.49	9.42	9.34
Na2O			5.87	5.79	5.88
K2O					
Total	100.46	100.79	101.25	100.71	101.02
Si	1.9774	1.9694	2.5675	2.5726	2.5752
Al	0.0541	0.0594	1.4318	1.4274	1.4272
Ti	0.0026	0.0033			
Fe	0.3583	0.3652	0.0074	0.0071	0.0048
Mn	0.0055	0.0058			
Mg	0.6631	0.6557			
Ca	0.9209	0.9274	0.4500	0.4488	0.4438
Na	0.0218	0.0224	0.5035	0.4996	0.5054
K			0.0156	0.0151	0.0143
Total	4.0036	4.0085	4.9758	4.9707	4.9707

plagioclase and quartz. A clinopyroxene next to orthopyroxene occurs in the left of the sketch. To avoid the effect of possible resetting at the waning stage of metamorphism, orthopyroxenes which are not in contact with other mafic minerals are used. A garnet in the middle shows a noticeable compositional variation. A compositional map of that garnet is shown in (b) of Fig. 3-3. Fe/(Fe+Mg) varies widely across the whole grain. Contours are dense near the contact with orthopyroxene. Truncation of contours are observed on the left side of the map. Fe ratio increases toward the rim, which gives the evidence of resetting during retrograde stage. Because there is no broad plateau in the middle of the garnet, it is hard to tell whether the core preserves the composition attained at the peak of metamorphism.

P-T conditions were determined with garnet-pyroxenes thermobarometry. Mineral compositions are listed in Table V. Numbers indicating each coexisting mineral calibration are the same as in sample Ar003-1a (Fig. 3-2 (a), (b)). The P-T conditions estimated from garnet-orthopyroxene thermobarometers, shown Fig. 3-4 (a), is in the range of 620 - 670° C, 5.6 - 6.3 kb. With garnet-clinopyroxene systems, 640 - 670°C, 4.7 - 5.7 kb was obtained for the maximum estimate of T and P (in Fig. 3-4 (b)). Calibration by Pattison & Newton (1989) gives a lower value by 40 - 100°C than other garnet-clinopyroxene thermometers.

3.4.3 Sample Ar003-1c

This is an example of the case where the mafic minerals are not in contact with each other. Therefore, we may assume that there were no exchange reactions during cooling. As shown in Fig. 3-5, mafic minerals are separated by matrixes of plagioclase and quartz. Mineral compositions are given in Table VI. The results of P-T condition from garnet-orthopyroxene, garnet-clinopyroxene thermobarometers are shown in Fig. 3-6 (a) and (b), respectively. Because there are some variations in the composition of

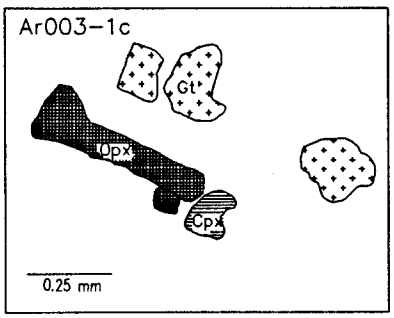

Fig. 3-5. A schematic sketch of sample Ar003-1c.

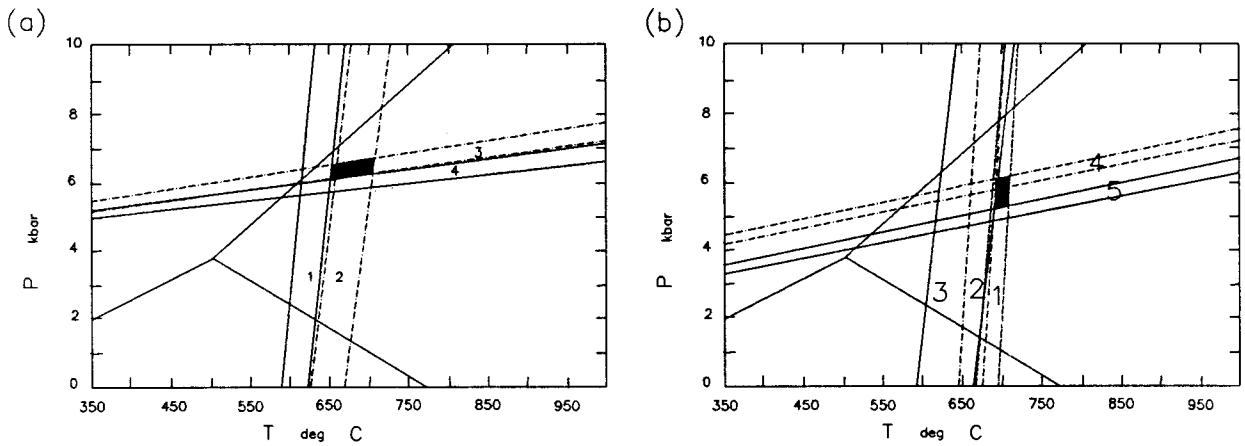

Fig. 3-6. P-T diagrams showing P-T conditions determined with garnet-orthopyroxene, garnet-plagioclase-orthopyroxene-quartz thermobarometers (a) and garnet-clinopyroxene, garnet-plagioclse-clinopyroxene-quartz thermobarometers (b). Numbers can be referred to Fig. 3-2.

Table VI. The compositions of the minerals of sample Ar003-1c.

	Garnet			Orthopyroxene		clinopyroxene		Plagioclase		
SiO2	38.82	38.83	38.64	51.67	51.28	52.44	51.95	58.22	57.95	58.52
Al2O3	21.60	21.83	21.82	0.80	0.81	1.42	1.79	27.30	27.09	27.24
TiO2				0.10	0.03	0.21	0.24			
FeO	28.30	28.45	28.58	30.34	30.20	12.81	11.81	0.10	0.10	0.12
MnO	1.56	1.60	1.55	0.54	0.58	0.27	0.26			
MgO	3.86	3.90	4.12	16.49	16.51	11.86	11.42			
CaO	7.46	7.40	7.23	0.68	0.57	21.61	23.33	9.46	9.31	9.30
Na2O						0.37	0.38	5.92	6.01	6.14
K2O										
Total	101.60	102.02	101.94	100.63	99.99	100.99	101.18	101.21	100.71	101.48
Si	3.0140	3.0030	2.9925	1.9864	1.9848	1.9684	1.9493	2.5761	2.5780	2.5819
Al	1.9764	1.9902	1.9911	0.0363	0.0372	0.0630	0.0791	1.4238	1.4203	1.4166
Ti				0.0030	0.0010	0.0059	0.0069			
Fe	1.8370	1.8403	1.8509	0.9754	0.9775	0.4021	0.3704	0.0037	0.0036	0.0043
Mn	0.1028	0.1050	0.1016	0.0176	0.0192	0.0085	0.0081			
Mg	0.4465	0.4492	0.4751	0.9453	0.9524	0.6636	0.6388			
Ca	0.6207	0.6136	0.6001	0.0281	0.0234	0.8689	0.9376	0.4485	0.4436	0.4398
Na				0.0002		0.0270	0.0274	0.5079	0.5185	0.5249
K										
Total	7.9973	8.0013	8.0114	3.9923	3.9954	4.0074	4.0176	4.9713	4.9777	4.9763

the garnets, there is about 100°C difference at the same pressure. Values of 650 - 710°C, 6.0 - 6.8 kb, and 690 - 710°C, 5.3 - 6.3 kb are inferred for the highest P-T conditions with the garnet-orthopyroxene and garnet-clinopyroxene systems, respectively.

3.5 Discussion.

Table VII shows the P-T conditions estimated from three different sections of sample Ar003-1. The resultant ranges of P-T conditions using two geothermobarometry relations are drawn in Fig. 3-7. For each box in that figure, the four boundaries are the results of four different calibrations. The upper and lower limits of temperature with garnet-orthopyroxene thermometer are from the relations of Sen & Bgattachaya (1984) and Harley (1984), respectively. The upper and lower limits of pressure obtained by the garnet-plagioclase-orthopyroxene-quartz barometer are from Newton & Perkins (1982) and Powell & Holland (1988). With the garnet-clinopyroxene thermometer, the two boundaries are from Ellis & Green (1979) and Powell (1985). As in the garnet-plagioclase-orthopyroxene-quartz barometer, the limits of pressure for the garnet-plagioclase-clinopyroxene-quartz barometer were obtained from Newton & Perkins (1982) and Powell & Holland (1988).

Different P-T conditions were obtained from the three different sections, though they are close to each other. It is possible to think that they record different stages of the retrogressive path of the metamorphism. The lowest temperature for the garnet-orthopyroxne thermometer was obtained from Ar003-1a. Considering the small inclusion of orthopyroxene in the garnet, it is natural to have a lower temperature than others. The highest temperature is from sample Ar003-1c in which the two minerals are apparently not in contact so that cation exchange during cooling is unlikely. The P-T conditions of Ar003-1b also are lower than that of Ar003-1c, implying chemical

Table VII. The P–T conditions determined with garnet–pyroxenes thermobarometry from a sample Ar003–1.

thermobarometer \ Sample	Ar003–1a	Ar003–1b	Ar003–1c
garnet–orthopyroxene thermometer	590 – 630 (°C)	620 – 670 (°C)	650 – 710 (°C)
garnet–plagioclase–orthopyroxene–quartz barometer	5.5 – 6.2 kb	5.6 – 6.2 kb	6.0 – 6.8 kb
garnet–clinopyroxene thermometer	680 – 700 (°C)	640 – 670 (°C)	690 – 710 (°C)
garnet–plagioclase–clinopyroxene–quartz barometer	5.3 – 6.3 kb	4.7 – 5.7 kb	5.3 – 6.3 kb

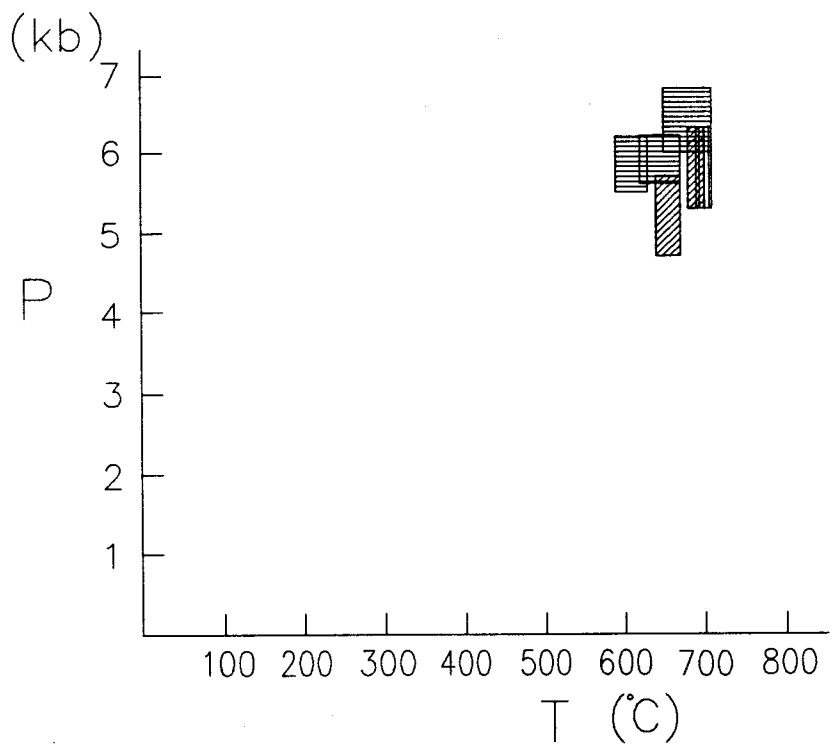

Fig. 3–7. A P–T diagram showing the ranges of P–T conditions from garnet–orthopyroxene(clinopyroxene) thermometer and garnet–plgioclase–orthopyroxene(clinopyroxene) barometer.
Upper three boxes are from garnet–orthopyroxene thermobarometry and lower three boxes are from garnet–clinopyroxene thermobarometry.

exchange with cooling. Even if the highest temperature from both thermometers coincide, it is not safe to say that it is the temperature of the peak metamorphism. With reference to the mineral assemblage of garnet-sillimanite-biotite-k-feldspar-quartz, a temperature of approximately 700°C can be considered as that of granulite facies.

If a temperature of about 710°C is estimated as close to the peak metamorphic conditions in the study area, this temperature is far from the highest estimated for the whole Highlands. However this result is closer to Bohlen's study (1985) than de Waard's. It is dangerous to speculate further about the cooling path of the rocks used in the present study. Assuming that the P-T conditions estimated from the three different sections of one thin-section record slightly different stages of the retrogressive path of the metamorphism, the path is not one of the isobaric cooling. However, it is not certain that this approach can be used to infer a cooling-path. Nevertheless it is interesting to notice that both cooling-paths from the garnet-orthopyroxne and garnet-clinopyroxene thermobarometers have a similar pattern, excluding the differences in the pressure estimates.

There is a greater uncertainty in the estimation of the pressure. Apparently, the pressure estimate determined by the garnet-plagioclase-orthopyroxene-quartz barometer is higher than that by the garnet-plagioclase-clinopyroxene-quartz barometer. It is not clear which results are better. In comparison with other barometers, the garnet-plagioclase-orthopyroxene-quartz barometry gives pressure estimates that are closer to those by others. The broad range of pressure estimated here also falls within the results of Bohlen et al. (1985).

I also examined some thin sections of the metapelitic rocks from the Southern Adirondacks and near the Brant Lake. They showed the same mineral assemblages as the metapelitic rocks of the Lake George Area. The mineral assemblages of these rocks are typical of the K-feldspar-sillimanite zone, which usually corresponds to the lower granulite facies. This could mean that the peak metamorphic condition was rather

uniform throughout the Southern and Southeast Adirondacks. Some metapelitic rocks are also known to exist in the central Highlands. Unfortunately, I did not have access to thin sections of those rocks. It would be interesting to compare the mineral assemblages from two distant parts of the Adirondacks.

Some questions remain in the interpretation of the geothermobarometry as to the accuracy and precision of the determination of the P-T conditions. For the Fe-Mg exchange thermometers, the precision is generally regarded to be ±20-30^{o}C at a given pressure. For barometers based on the coexistence of garnet and plagioclase, the precision is believed to generally be of the order of ±300-500 bars at a given temperature (Spear, 1989). The accuracy is much harder to evaluate because it comes from many factors such as the accuracy of the calibrations, activity-composition relations, and also the accuracy of the electron microprobe analyses.

CHAPTER 4. THERMOCHRONOLOGY FROM $^{40}Ar/^{39}Ar$ DATING METHOD

4.1 Analytic Procedures.

$^{40}Ar/^{39}Ar$ thermochronology has been widely used to infer the cooling history of rocks after major metamorphism. Four minerals from the Lake George Area were analyzed and dated with Ar isotopes technique. Hornblendes, biotite and microcline, sized to between 0.5mm and 0.75mm in diameter, were separated by conventional heavy liquid and magnetic separatory techniques. The mineral separates were handpicked to remove composite grains and other impurities, and therefore mineral separates were of great purity. The samples were irradiated with flux monitor at the Ford Reactor at the University of Michigan. Argon isotopic analyses were carried out on a Nuclide 4.5-60-RSS mass spectrometer (State University of New York at Albany). For detailed experimental procedures the reader is referred to Harrison and Fitz Gerald (1986).

4.2 Results.

Two step heating runs of the hornblendes from Amphibolite (Ar019-2) and Olivine metagabbro (Ar085-1) are shown in Fig. 4-1. The isotopic results for the samples are presented in Table VIII. The amphibolite hornblende Ar019-2 yields a plateau age of 971±5(1σ) Ma and the other gives a plateau age of 945±6 Ma. An unreasonably old age was obtained at the first step of heating of sample Ar085-1, which indicates the presence of excess ^{40}Ar. The age difference between these two hornblendes from different lithologies at different localities is 26 Ma. The age discrepancies from the same minerals in the same outcrop (central Adirondacks) has been reported by Onstott and Peacock (1987). Higher Fe/(Fe+Mg+Mn) in hornblende is correlated with younger ages. Representative microprobe analyses of hornblendes are

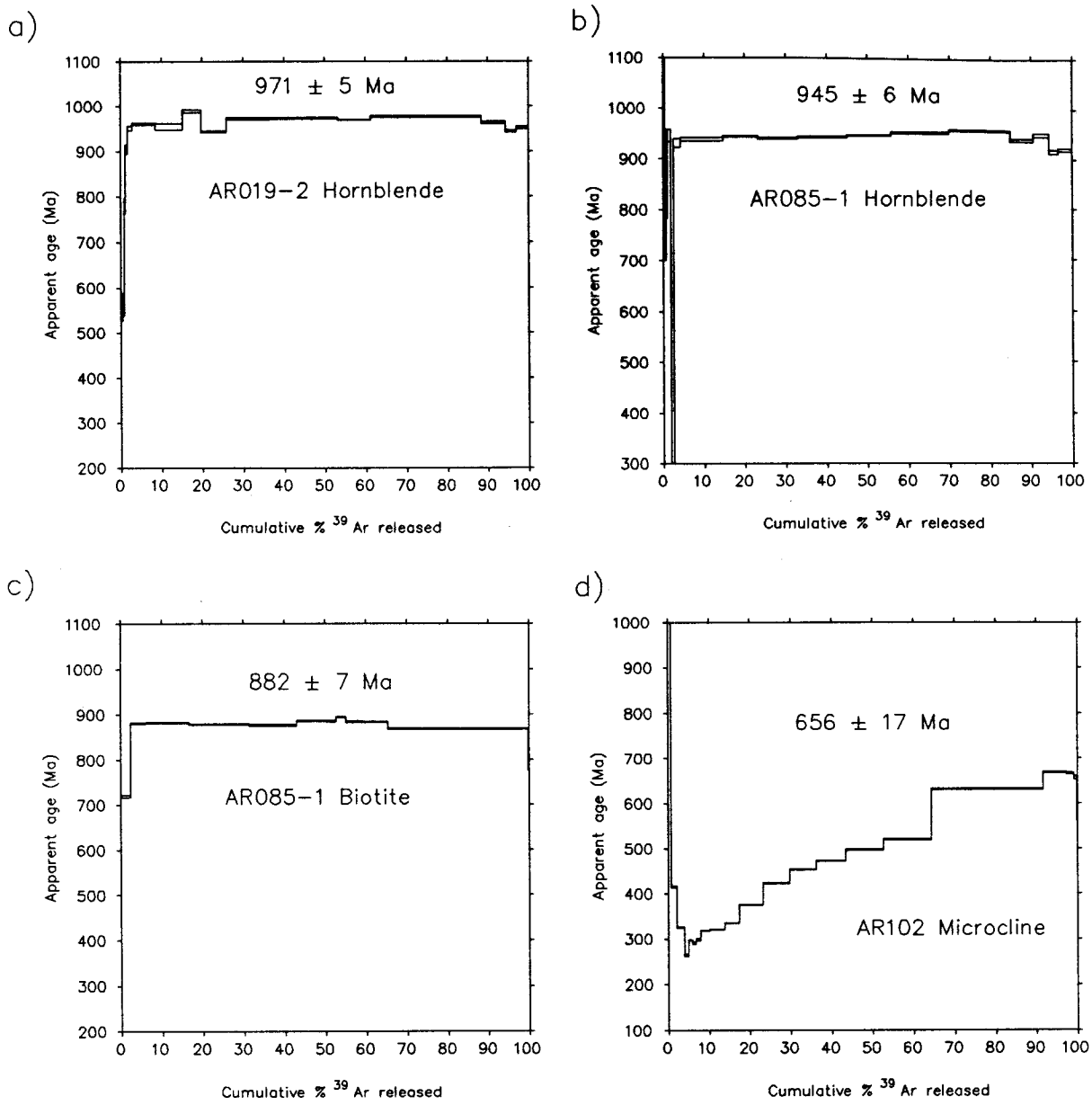

Fig. 4–1. $^{40}Ar/^{39}Ar$ age spectra of hornblendes, biotite and microcline from the Lake George Area.

Table VIII. Anaytical data of argon isotopes from step-heating experiments on samples from the Lake George Area

Temp C	40Ar/39Ar	37Ar/39Ar	36Ar/39Ar (E-3)	39Ar (E-13 mol)	%39Ar released	40Ar* %	40Ar*/39Ark	AGE + 1 s.d. Ma
a) Ar 019-2 Hornblende (J = 0.005025; wt. = 0.10596g)								
750	350.50	1.354	952.800	0.134	0.514	19.6	69.05	537.4 + 10.5
900	89.37	3.632	56.950	0.086	0.843	80.3	72.93	563.3 + 25.0
950	117.40	6.503	36.070	0.099	1.230	90.5	107.70	780.1 + 16.9
970	130.40	5.154	5.436	0.122	1.700	98.4	129.50	904.5 + 10.3
1010	140.80	3.345	10.350	0.304	2.870	97.7	138.30	951.8 + 4.3
1040	140.70	2.940	3.876	1.470	8.540	99.2	140.00	960.9 + 2.8
1060	139.40	2.913	3.141	1.720	15.200	99.4	139.00	955.4 + 7.4
1080	145.50	3.100	2.205	1.170	19.700	99.6	145.40	989.4 + 3.3
1100	137.40	2.844	3.956	1.610	25.900	99.2	136.70	943.3 + 1.9
1120	142.70	2.934	3.050	2.810	36.700	99.4	142.20	972.9 + 2.5
1140	142.50	2.946	2.515	4.300	53.200	99.6	142.20	972.6 + 1.8
1160	141.80	2.924	2.424	2.100	61.300	99.6	141.50	969.1 + 1.1
1180	142.90	2.951	1.342	7.050	88.400	99.8	143.00	976.8 + 1.3
1200	140.50	2.925	1.332	1.560	94.400	99.8	140.50	963.9 + 2.5
1220	138.30	2.937	6.162	0.693	97.000	98.7	136.90	944.3 + 3.0
1450	139.30	3.156	5.089	0.769	100.000	98.9	138.30	951.8 + 2.6
b) Ar085-1 Hornblende (J = 0.00502; wt. = 0.17741g)								
750	509.50	3.557	825.600	0.086	0.430	52.000	266.40	1532 + 23.1
850	113.90	4.183	48.140	0.073	0.796	86.700	100.20	735.1 + 35.1
900	138.20	3.889	82.390	0.044	1.020	81.200	114.40	818.7 + 35.5
950	143.30	3.872	22.110	0.174	1.890	95.200	137.40	946.1 + 12.9
970	19.55	3.760	7.450	0.135	2.560	86.500	17.60	152.7 + 37.2
990	135.50	3.772	4.950	0.339	4.260	98.800	134.60	931.1 + 8.7
1010	136.70	3.970	4.963	2.080	14.700	99.000	135.80	938.0 + 3.3
1030	137.50	4.021	4.085	1.690	23.200	99.200	136.90	943.9 + 1.3
1050	136.90	4.045	4.577	1.950	32.900	99.100	136.20	940.0 + 1.6
1070	136.90	4.040	3.113	2.410	45.000	99.500	136.60	942.2 + 1.5
1090	137.20	4.051	2.470	2.130	55.700	99.600	137.10	944.6 + 1.2
1110	138.10	4.013	2.396	2.830	69.900	99.600	138.00	949.7 + 1.7
1130	139.00	4.025	2.025	2.980	84.800	99.700	139.10	955.3 + 1.5
1150	136.20	3.944	3.813	1.140	90.500	99.300	135.70	937.2 + 2.7
1180	138.00	4.033	2.612	0.748	94.300	99.500	137.80	948.7 + 3.2
1210	134.00	4.019	9.923	0.464	96.600	997.800	131.60	915.2 + 4.2
1450	136.10	3.806	14.830	0.674	100.000	96.800	132.30	919.0 + 2.7
c) Ar085-1 Biotite (J = 0.005015; wt. = 0.07606g)								
600	131.90	0.0187	115.6000	0.884	2.430	74.000	97.71	719.5 + 2.6
680	129.90	0.0350	14.4700	1.390	6.250	96.600	125.50	881.0 + 0.9
750	126.80	0.0228	3.2990	3.830	16.800	99.200	125.80	882.2 + 1.4
800	125.30	0.0050	0.3919	5.350	31.500	99.900	125.10	878.7 + 1.2
840	125.60	0.0184	2.9270	4.200	43.000	99.300	124.70	876.3 + 1.3

Table VIII (Continued)

Temp C	40Ar/39Ar	37Ar/39Ar	36Ar/39Ar (E-3)	39Ar (E-13 mol)	%39Ar released	40Ar* %	40Ar*/39Ark	AGE + 1 s.d. Ma
900	126.60	0.0098	0.3282	2.680	50.400	99.900	126.40	886.0 + 1.3
950	126.60	0.0140	0.4259	0.805	52.600	99.800	126.40	885.7 + 1.5
1000	128.10	0.0114	0.8490	0.870	55.000	99.700	127.80	893.7 + 1.6
1050	126.80	0.0296	1.9870	1.390	58.800	99.500	126.10	884.3 + 1.3
1100	126.30	0.0240	1.0060	2.340	65.300	99.700	126.00	883.6 + 1.5
1200	123.80	0.0224	1.6370	12.500	99.700	99.600	123.30	868.6 + 1.0
1350	111.20	0.0614	10.3000	0.119	100.000	96.500	108.10	781.4 + 4.2
		d) Ar102 Microcline (J = 0.00501; wt. = 0.07085g)						
500	403.10	0.0109	31.8200	0.143	0.174	97.5	393.60	1965 + 8.2
550	156.30	0.0517	9.6520	0.424	0.689	98.0	153.40	1029 + 4.9
600	52.46	0.0208	3.0110	1.010	1.910	98.1	51.54	414.4 + 1.9
650	40.04	0.0302	1.8680	1.260	3.440	98.3	39.46	325.4 + 1.4
680	32.39	0.0362	3.0900	0.807	4.420	96.7	31.44	263.9 + 2.3
710	35.86	0.0162	0.3653	0.676	5.240	99.2	35.72	297.0 + 1.6
740	35.72	0.0304	2.7600	0.639	6.020	97.2	34.87	290.5 + 2.3
770	36.12	0.0269	0.5106	0.832	7.030	99.2	35.94	298.7 + 2.7
820	38.68	0.0345	0.3758	1.600	8.970	99.5	35.54	318.5 + 0.7
870	39.17	0.0182	0.9525	2.650	12.200	99.1	38.85	320.9 + 1.0
920	40.81	0.0151	0.5013	2.600	15.300	99.5	40.63	334.3 + 0.6
970	46.38	0.0112	0.6472	4.190	20.400	99.5	46.15	375.3 + 0.7
1020	53.00	0.0195	0.7922	4.690	26.100	99.5	52.73	422.9 + 1.0
1050	57.27	0.0127	0.8837	4.710	31.800	99.4	56.97	453.0 + 0.7
1080	60.12	0.0191	1.3230	5.160	38.100	99.3	59.70	472.0 + 1.0
1120	63.71	0.0239	1.3460	6.670	46.200	99.3	63.28	496.8 + 0.9
1150	67.12	0.0294	1.6460	8.490	56.500	99.2	66.69	520.1 + 1.1
1200	0.00	0.0000	0.0000	10.000	68.700	0.0	0.00	0.0 + 0.0
1240	84.14	0.0154	1.5090	19.700	92.600	99.4	83.66	635.1 + 1.0
1280	90.31	0.0233	2.3390	4.160	97.700	99.2	89.59	668.9 + 1.0
1350	90.53	0.0241	4.1240	1.330	99.300	98.5	89.28	667.0 + 2.0
1450	108.00	0.0875	68.6400	0.446	99.800	81.0	87.70	657.0 + 3.4
1520	113.70	0.0714	127.2000	0.124	100.000	66.4	76.07	582.5 + 20.5

given in Table IX. The compositional differences are relatively small. Sample Ar085-1, with a slightly younger age, has a slightly higher Fe/(Fe+Mg) ratios. Greater variation in composition was revealed by microprobe analyses in that sample. This may suggest some variation in closure temperatures in hornblendes. The closure temperature of the hornblende with higher Fe ratio is lower than that with lower Fe ratio. But the two samples are almost 8 miles apart so that the indicated age difference could be real.

Biotite from an olivine metagabbro (Ar085-1) yields a plateau age of 882±7 Ma from step heating technique (Fig. 4-1c). The age spectrum shows a flat release pattern. Apparent ages increase from 719 Ma in the lowest temperature step to a regular plateau with an age of about 880 Ma.

Figure 4-1d is an age spectrum of microcline from metapelite Ar102. It shows a gradual increase in ages up to 70% of ^{39}Ar release and then average flat age of 656±17 Ma. This shape of release pattern may be due to slow cooling, or episodic loss at 200 Ma as suggested by Heizler (1986) from a wider study of the K-feldspars of the Adirondacks. An Arrhenius plot (Fig. 4-2) showing diffusion of argon in microclines makes it possible to calculate diffusion parameters. The data (Table X), for extraction temperatures from 740^{o} C to 1150^{o} C, yields a linear array on an Arrhenius plot, corresponding to an activation energy (E) of about 30 Kcal/mol and 3/sec of a Do/l^2. These values are close to those of Harrison and McDougall (1982). From the following equation of Dodson (1973), the closure temperature (T_C) can be calculated;

$$Tc = \frac{E/R}{\ln[ART_C^2(D_O/l^2)/E\ (dT/dt)]}$$

where R is the gas constant, E the activation energy, T_C is the closure temperature, A is the numerical constant, D_O is the diffusion coefficient, l is the characteristic diffusion radius, and dT/dt is the cooling rate. A closure temperature of about 140^{o} C was obtained assuming a plane sheet geometry and cooling rate of 1^{o} C/Ma.

Table IX. Representative compositions of hornblendes from electron microprobe analyses.

	AR019-2		AR085-1	
SiO2	42.56	42.62	41.8	41.96
Al2O3	11.11	11.1	12.48	12.54
TiO2	2.01	2.08	2.19	1.94
MgO	9.23	9.19	8.74	9.19
FeO	17.74	17.76	18.39	18.26
MnO	0.19	0.2	0.17	0.16
CaO	11.67	11.53	10.65	10.84
Na2O	2.16	2.16	2.15	2.29
K2O	1.48	1.49	1.26	1.24
Total	98.16	98.14	97.83	98.41
Fe/(Fe+Mg)	0.52	0.52	0.54	0.53
K/Ca	0.15	0.16	0.14	0.14

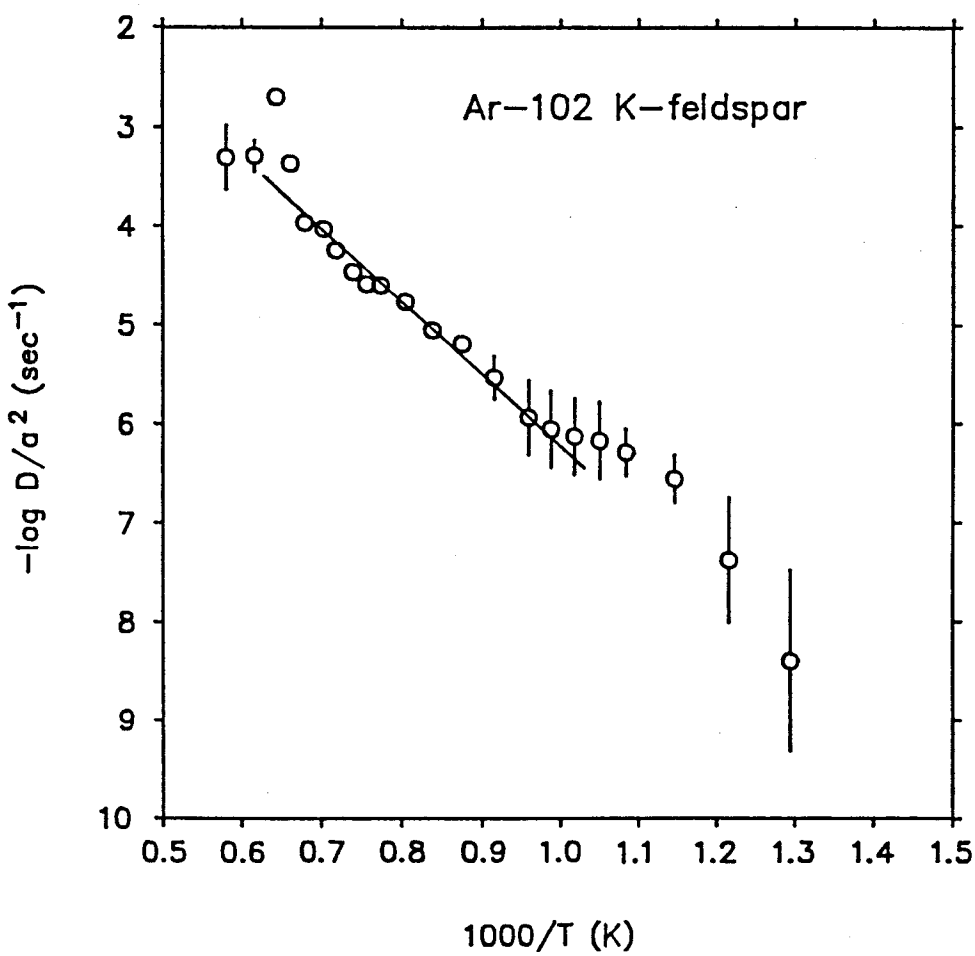

Fig. 4-2. Arrhenius plot of -log D/l^2 values versus the reciprocal absolute temperature of the extraction step for sample Ar102.

Table X. Calculated parameters for Arrhenius plots using a plane sheet geometry for microcline (sample Ar 102).

Temp C	Time Min	f	Dt/l^2	Residual/t	1000/t (k)	-LOG(D/l^2)
500	10	0.0017	2.367E-06	3.959E-09	1.294	8.402
550	14	0.0069	3.723E-05	4.164E-08	1.215	7.381
600	15	0.0191	2.862E-04	2.774E-07	1.145	6.557
650	21	0.0344	9.305E-04	5.127E-07	1.083	6.290
680	15	0.0442	1.535E-03	6.735E-07	0.149	6.172
710	14	0.0524	2.158E-03	7.429E-07	1.017	6.129
740	13	0.0602	2.844E-03	8.821E-07	0.987	6.054
770	15	0.0703	3.878E-03	1.152E-06	0.959	5.938
820	14	0.0897	6.319E-03	2.913E-06	0.915	5.536
870	14	0.1219	1.167E-02	6.387E-06	0.875	5.195
920	13	0.1535	1.850E-02	8.766E-06	0.838	5.057
970	14	0.2043	3.278E-02	1.703E-05	0.805	4.769
1020	14	0.2613	5.361E-02	2.485E-05	0.773	4.605
1050	17	0.3185	7.963E-02	2.555E-05	0.756	4.593
1080	17	0.3811	1.140E-01	3.380E-05	0.739	4.471
1120	16	0.4621	1.677E-01	5.595E-05	0.718	4.252
1150	15	0.5652	2.508E-01	9.255E-05	0.703	4.034
1200	21	0.6867	3.852E-01	1.069E-04	0.679	3.971
1240	23	0.9264	9.723E-01	4.260E-04	0.661	3.371
1280	12	0.9769	1.442E+00	2.005E-03	0.644	2.698
1350	16	0.9931	1.930E+00	5.095E-04	0.616	3.293
1450	21	0.9985	2.549E+00	4.915E-04	0.580	3.308

4.3 A Cooling History of the Southeastern Adirondacks.

If the mineral ages and closure temperatures for individual minerals are known, the cooling history can be inferred. There have been many dates published in establishing age of the Grenville Orogeny. Zircon ages of 1020-1200 Ma of Silver (1969) and a Sm-Nd age of 1095±7 Ma from Basu & Pettingill (1983) were obtained for the granulite facies metamorphism. Application of the Sm-Nd method to the anorthosite massif (Ashwal and Wooden, 1983) suggested that the metamorphic event extended 950-1200 Ma ago. From the Lake George Area, an age of 1071±20 m.y. was obtained for the Grenville metamorphism by the rubidium-strontium whole-rock method (Hills and Gast, 1964). Results of the U-Pb mineral ages from garnet, monazite and sphene indicate that high-grade metamorphic conditions lasted from about 1154 to 1000 Ma (Mezger, Bohlen and Hanson, 1988, 1989). Among these numerous dates of the metamorphism, it would be unrealistic to choose one date for the time of the peak metamorphism, because the metamorphism could last for a long time. Also different methods of dating are subject to various closure temperatures which are not precisely known. Even though there is wide range of the ages published for the time of the metamorphism, many of them cluster around 1100-1000 Ma. From the reviews of mineral dates from the Grenville Orogenic Belt, it has been suggested that the peak metamorphism occurred not much earlier than 1100 Ma ago (Anderson, 1988). The value of 710^{o} C has been assumed as the condition of the peak metamorphism for the Lake George Area.

The closure temperatures of argon diffusion for the minerals used in the present study are 500^{o} C (Harrison and McDougall, 1980b), 300^{o} C (Harrison, Duncan and McDougall, 1985) and 140^{o} C (from present study) for hornblende, biotite, and microcline, respectively. The average cooling rate from the peak of metamorphism to closure temperature of argon in hornblende is about 2.7^{o} C/Ma (1050 Ma was taken as the time of peak metamorphism). The difference in hornblende-biotite ages corresponds

to an average cooling rate of 2.2° C/Ma. The ages of biotite and microcline lead to a cooling rate of 0.7° C/Ma for the closure temperature interval of biotite and microcline. After the closure of argon in microcline, the cooling rate of the Southeast Adirondacks has been very slow. Figure 4-3 shows a possible cooling path for the Lake George Area based on the mineral ages determined in this study.

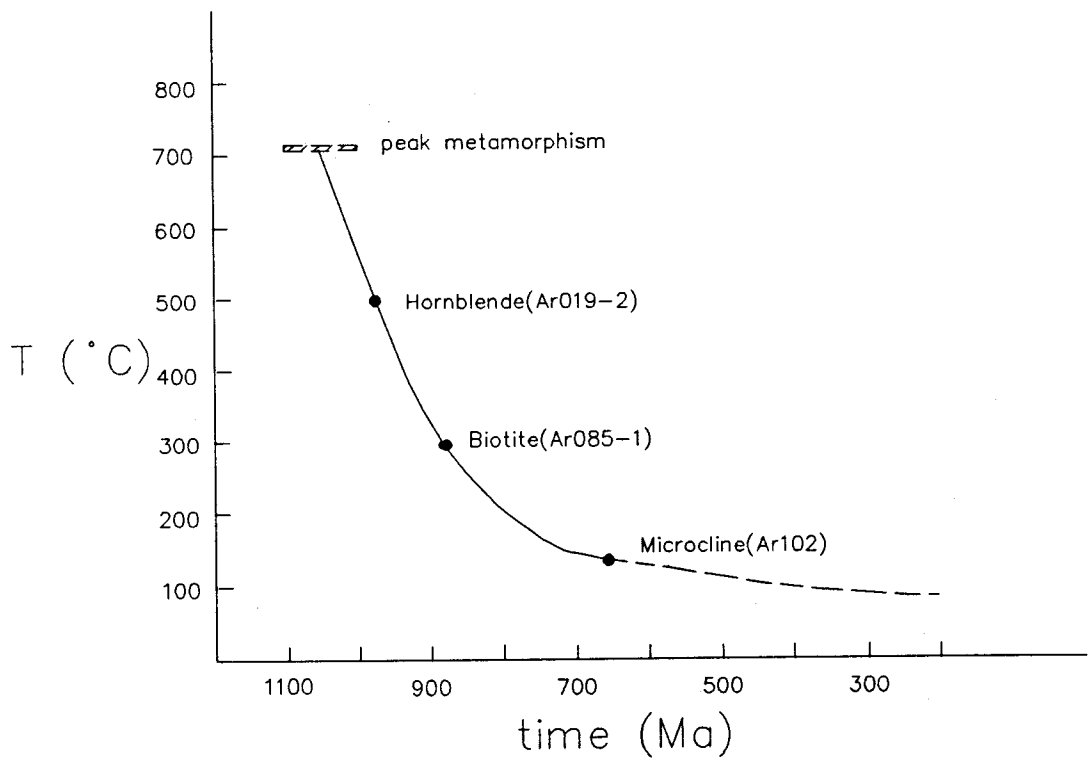

Fig. 4-3. A possible cooling path drawn with $^{40}Ar/^{39}Ar$ mineral dates for the Lake George Area.

CHAPTER 5. CONCLUSION AND SUMMARY

The metamorphosed rocks of the Lake George Area were derived partly from a range of igneous rocks and partly from sedimentary rocks. They show a variation in mineral assemblages. Excluding minerals of retrogressive origin, the mineral assemblages of all metamorphic rocks can be assigned to the same metamorphic facies, that is, a lower-grade part of the granulite facies. The observed variations in mineral assemblages may be explained by differences in bulk-composition. Although it is not possible to prove this positively, there are no inconsistent mineral assemblages to conflict to this idea.

The estimated highest temperature of 710°C is consistent with the observed mineral assemblages of a lower-grade part of the granulite facies. Thus it may represent the temperature of the thermal peak, although this cannot be positively proven.

The following statements are the summaries and conclusions from the previous chapters.

1. A subdivision of the granulite facies which was proposed by de Waard (1965) is not applicable to the rocks of the Lake George Area.

2. The CFM diagram of Abbott (1982) was tested to show the relationship between composition and paragenesis of the rocks of the Lake George Area.

3. From the analyses of minerals of various rock types, the observed order of X_{Fe} of coexisting minerals is somewhat different from that of Abbott; garnet>hornblende>biotite≥orthopyroxene>clinopyroxene.

4. According to Abbott's subdivision of the granulite facies the hornblende granitic gneiss belongs to a different subfacies from the mafic granulite and charnockitic gneiss. But, if the order of X_{Fe} of coexisting minerals observed in this study is used, the mineral assemblage of the hornblende granitic gneiss need not be considered to belong to a different subfacies from other rocks of this area.

5. From the zoning profiles of elements in garnets of the biotite-garnet-sillimanite gneiss, it is suggested that the composition of the core of garnet has probably been erased by diffusion at high temperature.

6. The biotites of metapelite in the Lake George Area show a different substitution mechanism from those of other regions of the granulite facies.

7. The P-T conditions were estimated from mineral assemblages in three different parts of one thin section. The results show variation wherein the maximum estimate was obtained for the part where the relevant mafic minerals were not in contact with one another.

8. The highest estimate of temperature condition (about 710° C) appears to be consistent with the isotherm pattern of Bohlen et al. (1985) as it applies to the Lake George Area.

9. Mineral ages via the $^{40}Ar/^{39}Ar$ method were performed to infer the cooling history of the Southeast Adirondacks. Plateau ages of 971±5(1σ), 882±7 and 656±17 Ma were determined for hornblende. biotite and microcline, respectively.

10. With these mineral ages and appropriate closure temperatures for each mineral, average cooling rates of 2.7° C/Ma, 2.2° C/Ma, and 0.7° C/Ma for the time intervals from peak metamorphism-hornblende, hornblende-biotite, and biotite-microcline closures, respectively, were determined.

REFERENCES

Abbott, R.N., Jr., 1982, A petrogenetic grid for medium and high grade metabasites, American Mineralogist, v. 67, 865-876.

Alling, H.L., 1918, The Adirondack graphite deposits, N.Y. State Musium Bulletin, 199.

Anderson, S.L., 1988, Interpretation of K-Ar mineral dates from the Grenville Orogenic Belt, American Journal of Science, v. 288, 701-734.

Ashwal, L.D., Wooden, J.L., 1983, Sm and Nd isotopic geochronology, geologic history, and origin of the Adirondack Anorthosite, Geochemica Cosmochemica Acta 47, 1875-1885.

Basu, A.R., Pettingill, H.S., 1983, Orgin and age of Adirondack anorthosites re-evaluated with Nd isotopes, Geology, 11, 514-518.

Bence, A.E., Albee, A.L., 1968, Empirical correction factors for the electron microanalysis of silicates and oxides, Journal of Geology, 76, 382-404.

Bickford, M.E., Turner, B.B., 1971, Age and probable anatectic origin of the Brant Lake Gneiss, Southeastern Adirondacks, New York: Geological Society of America Bulletin, v. 82, no. 8, 2333-2342.

Bohlen, S.R., 1983, Retrograde P-T paths for granulites, EOS, v. 64, no. 45, 878.

Bohlen, S.R., 1987, Pressure - Temperature - time paths and a tectonic model for the evolution of granulites, Journal of Geology, v. 95, 617-632.

Bohlen, S.R., Essene, E.J., 1977, Feldspar and oxide thermometry of granulites in the Adirondack Highlands, Contribution to Mineralogy and Petrology, v. 62, 153-169.

Bohlen, S.R., Essene, E.J., 1980, Evaluation of coexisting garnet-biotite, garnet-clinopyroxene, and other Mg-Fe exchange thermometers in Adirondack granulites: Summary, Geological Society of America Bulletin, Part I, v.91, 107-109.

Bohlen, S.R., Essene, E.J., Hoffman, K.S., 1980, Update on feldspar and oxide thermometry in the Adirondack Mountains, New York, Geological Society of America Bullitin, Part I, v.91, 110-113.

Bohlen, S.R. et al, 1983, Experimental investigation and application of garnet granulite equilibria, Contribution to Mineralogy and Petrology, 83,52-61.

Bohlen, S. R., 1987, Pressure - temperature - time paths and a tectonic model for the evolution of granulites, Jour. of Geology, v. 95, 617-532.

Bohlen, S.R. et al., 1985, Metamorphism in the Adirondacks, I. Petrology, pressure and temperature, Journal of Petrology, v. 26, part 4, 971-992

Bohlen, S.R. and Essene, E.J., 1980, Evaluation of coexisting garnet-biotite, garnet-clinopyroxene and other Mg-Fe exchange thermometers in Adirondack granulites, Geological Society of America Bulletin, part II, v. 91, 659-684.

Buddington, A.F., 1939, Adirondack igneous rocks and their metamorphism, Geological Society of America Memoir 7, 354p.

Buddington, A.F., 1948, Origin of granitic rocks of the northwest Adirondack, Geological Society of America Memoir, 28, 21-43.

Buddington, A.F., 1963, Isograds and the role of H_2O in metamorphic facies of orthogneisses of the northwest Adirondack Area, New York, Geological Society of America Bulletin, v. 74, 1155-1182.

De Waard, D., 1965, A proposed subdivision of the granulite facies, American Journal of Science, v. 263, 455-461.

De Waard, D., 1965b, The occurrence of garnet in the granulite-facies Terrane of the Adirondack Highlands, Journal of Petrology, v. 6, part I, 165-191.

De Waard, D., 1971, Threefold division of the granulite facies in the Adirondack Moutains, Krystalinikum, 7, 85-93.

Dodson, M.H., 1973, Closure temperature in cooling geochronological and petrological systems, Contrib. Mineral. Petrol., 40, 259-257.

Dymek, R. F., 1983, Titanium, aluminum and interlayer cation substitions in biotite from high - grade gneisses, West Greenland, American Mineralogist, 68, 880-899.

Ellis, D. J. and Green, D.H., 1979, An experimental study of the effect of Ca upon garnet-clinopyroxene Fe-Mg exchange equilibria, Contrib. Mineral. Petrol., 71, 13-22.

Engel, A.E.J., Engel, C.G., 1958, Progressive metamorphism and granitization of the major paragneiss, northwest Adirondack Mountains, New York, Part I. Total rock. Ibid. 69, 1369-1414.

Engel, A.E.J., Engel, C., 1960, Progressive metamorphism and granitization of the major paragneiss, northwest Adirondack Mountain, New York, Geological Society of American Bulletin, v. 71, 1-58.

Engel, A.E.J., Engel, C., 1962, Progressive metamorphism of amphibolite, northwest Adirondack Mountains, New York, p. 37-74 in Engel, A.E.J., James, H.L., and Leonard, B.F., Editors, Petrologic Studies: Geological Society of America, Buddington Volume, 660p.

Eskola, P., 1939, Die metamorphen Gesteine, in Barth, T.F.W., Correns, C.W., and Eskola, Pentti, Die Enstehung der Gesteine: Berlin, Julius Springer, 263-407.

Fisher, D.W., 1984, Bedrock geology of the Glens Fall-Whitwhall Region, New York, New York State Museum map and chart series number 35.

Grant, S.M., 1988, Diffusion models for corona fromation in metagabbros from the western Grenville Province, Canada, Contribution to Meneralogy and Petrology, 98, 49-63.

Harley, S.L., 1984, An experimental study of the partitioning of Fe and Mg between garnet and orthopyroxene, Contrib. Mineral. Petrol., 86, 359-373.

Harrison, T.M., McDougall I., 1980b, Investingations of an intrusive contact, northwest Nelson, New Zealand - II: Diffusion of radiogenic and excess ^{40}Ar in

hornblende revealed by $^{40}Ar/^{39}Ar$ age spectrrum analysis, Geochimica et Cosmochimica Acta 44, 2005-2020.

Harrison, T.M., McDougall, I., 1982, The thermal significance of potassium feldspar K-Ar ages inferred from $^{40}Ar/^{39}Ar$ age spectrum results, Geochmica et Cosmochimica Acta 46, 1811-1820.

Harrison, T.M., Duncan I., McDougall, I., 1985, Diffusion of ^{40}Ar in biotite: Temperature, pressure and compositonal effects, Geochimica et Cosmochimica Acta 49, 2461-2468.

Harrison, T.M., Fitz Gerald, J.D., 1986, Exsolution in hornblende and its consequences for $^{40}Ar/^{39}Ar$ age spectra and closure temperature, Geochimica et Cosmochimica Acta 50, 247-253.

Heizler, M.T. and Harrison, T.M., 1986, The chronology of Adirondack epeirogeny (abstract), EOS Trans. Am. Geophys. Union, 67, 620.

Hills, A., Gast, P.W., 1964, Age of pyroxene-hornblende granitic gneiss of the eastern Adirondacks by the rubidium-strontium whole-rock method, Geological Society of America Bulletin, v. 75, 759-766.

Holdaway, M.J.,.1971, Stability of andalusite and the aluminum silicate phase diagram. American Journal of Science, 271, 97-131.

Joesten, R., 1986a, The role of magmatic reaction, diffusion and annealing in the evolution of coronitic mecrostructures in troctolitic gabbro from Risor, Norway, Mineral Magazine 50, 441-467.

Joesten, R., 1986b, Reply, Mineral Magazine 50, 474-479.

Lonker, S., 1980, Conditions of metamorphism in high-grade pelitic gneisses from the Frontenac Axis, Ontario, canada, Can. J. Earth Sci., v. 17, 1666-1684.

McLelland, J. and Isachsen, Y, 1980, Structural synthesis of the southern and cintral Adirondacks : A model for the Adirondacks as a whole and plate - tectonecs interpretations, Geol. Soc. of America Bulletin, part II, 192-207.

Mezger, K., Bohlen, S.R., and Hanson, G.N., 1988, U-Pb garnet, monazite and rutile ages: Implications for the duration of high-grade metamorphism and cooling histories, Adirondack Mts., N.Y., Geol. Soci. Am., Abstr. Progr. A100.

Mezger, K., Bohlen, S.R., and Hanson, G.N.,1989, High-precision U-Pb ages of metamorphic rutile: application to the cooling history of high-grade terranes, Earth and Planetary Science Letters, 96, 106-118.

Onstott, T.C., Peacock, M.W., 1987, Argon retentivity of hornblendes: A field experiment in a slowly cooled metamorphic terrane, Geochim. Cosmochim. Acta 51, 2891-2903.

Powell, R., 1985, Regression diagnostics and robust regression in geothermometer/geobarometer revisited, Jour. Met. Geol., 3, 231-243.

Powell, R. and Holland, T.J.B., 1988, An internally consistent thermodynamic dataset with uncertainties and correlations: 3. Applications to geobarometry, worked examples and a computer program. Journal of Metamorphic Geology. v. 6, 173-204.

Putman, G.W., Sullivan, J.W., 1979, Granitic pegmatites as estimators of crustal pressures - A test in the eastern Adirondacks, New York, Geology, v. 7, 549-553.

Raheim, A. and Green, D. H., 1974, Experimental determination of the temperature and pressure dependence of the Fe-Mg partition coefficient for coexistion garnet and clinopyroxene, Contrib. Mineral. Petrol., 48, 179-203.

Rivers, T., et al., 1989, New tectonic divisions of the Grenville Province, Southeast Canadian Shield, Tectonics, v. 8, no. 1, 63-84.

Schreurs, J., 1985, Prograde metapelites, garnet-biotite thermometry and prograde changes of biotite chemistry in high - grade rocks of West Uusimaa, Southwest Finland, Lithos, 18, 69-80.

Selleck, B.W., 1980, The post-orogenic history of the Adirondack Mountain region: A review, Geological Society of Americ Bulletin, Part I, v. 91, 120-124.

Sen, S. K. and Bhattacharya, A., 1984, An orthopyroxene - garnet thermometer and its application to the Madras charnockites, CMP, 88, 64-71.

Silver, L.T., 1969, A geochronologic investigation of the Adirondack Complex, Adirondack Mountains, New York, In: Isachsen Y.W.(ed.), Origin of Arothosite and Related Rocks. Mem. N.Y.St.Mus.Sci.Serv. 18, 233-252.

Spear, F.S., 1989, Petrologic determination of metamorphic Pressure-Temperature-time paths. In short course notes for IMA.

Thompson, J.B., Jr, 1957, The graphical analysis of mineral assemblages in pelitic schist, American Mineralogist, 42, 842-858.

Turner, F.J., 1958, Mineral assemblages of individual metamorphic facies. in Fyfe, W.S., Turner, F.J., and Verhoogen, John, Metamorphic reactions and metamorphic facies: Geol. Soc. America Mem. 73.

Turner, F.J., 1968, Metamorphic petrology, McGraw-Hill, New York.

Turner, B. B., 1980, Polyphase precambrian deformation and stratigraphic relations, central to southeasteern Adirondack Mountains, New York, Geological society of America Bulletin, part II, v. 91, 208-292.

Valley, J. W., 1988, Polymetamorphism in the Adirondacks : Wollastonite at the contacts of shallowly intruded anorthosite. In: Touret, J.L. (ed.) The Deep Proterozoic Crust in the North Atlantic Provinces. Reidel.

Walton, M.S. and De Waard, D., 1963, Orogenic evolution of the Precambrian in the Adirondack Highlands, a new synthesis, Koninkl. Nederl. Akadimie Van Wetenschappen - Amsterdam, Reprinted from Proceedings, Series B, 66, No. 3, 1963.

Wiener,R. W. et al., 1984, Stratigraphy and structural geology of the Adirondack Mountains, New York : Review and synthesis, Geol. Society of America, Special paper, 94, 1-55.

Whitney, P. R., 1978, The significance of garnet "isograds" in granulite facies rocks of the Adorondacks, Geol. Survey of Canada, Paper 78-10, 357-366

Whitney, P. R., 1983, A three-stage model for the tectonic history of the Adirondack region, New York, (New York State Museum, Science Service, Journal Series No. 411), Northeastern Geology, v. 5, no. 2, 61-72.

Whitney, P.R., McLelland, J.R., 1973, Origin of coronas in Metagabbros of the Adirondack Mts, N.Y., Contribution to Mineralogy and Petrology, 39, 81-98.

Whitney, P.R., McLelland, J.R.,1983, Origin of biotite-hornblende-garnet coronas between oxides and plagioclase in Olivine Metagabbros, Adirondack region, Mew York, Contribution to Mineralogy and Petrology, 82, 34-41.

Wood, B. J., 1975, The influence of pressure, temperature and bulk composition on the appearance of garnet in orthogneiss - an example from south Harris, Scotland, Earth and Planetary Science Letters, 26, 299-311.

APPENDIX

List of samples (in Fig. 1-2.) which are not shown in Table 1

Sam. no.	Rock type , description	Sam. no.	Rock type, description
14	granitic gneiss	74	mafic granulite
17	hornblende granitic gneiss	76	olivine metagabbro
19	amphibolite (pelitic)	78	granitic gneiss
20	charnockitic gneiss	80	biotite-garnet-sillimanite gneiss
21	biotite-quartz-plagioclase gneiss	81	leucogranitic gneiss
22	marble	83	hornblende granitic gneiss
24	biotite-quartz-plagioclase gneiss	92	hornblende granitic gneiss
25	biotite-quartz-plagioclase gneiss	95	leucogranitic gneiss
26	amphibolite	96	leucogranitic gneiss
27	biotite-quartz-plagioclase gneiss	97	mafic granulite
29	biotite-quartz-plagioclase gneiss	98	hornblende granitic gneiss
30	biotite-quartz-plagioclase gneiss	99	hornblende granitic gneiss
31	mafic granulite	100	mafic dyke
33	hornblende granitic gneiss	101	pegmatitic gneiss
35	quartzite	103	biotite-quartz-plagioclase gneiss
36	biotite-garnet-sillimanite gneiss	104	biotite-quartz-plagioclase gneiss
37	biotite-garnet-sillimanite gneiss	105	hornblende granitic gneiss
38	quartzite	106	biotite-quartz-plagioclase gneiss
39	mafic granulite	109	biotite-garnet-sillimanite gneiss
43	hornblende granitic gneiss	110	mafic granulite or charnockitic gneiss
45	biotite-garnet-sillimanite gneiss	111	biotite-quartz-plagioclase gneiss
46	biotite-garnet-sillimanite gneiss	112	charnockitic gneiss
49	biotite-quartz-plagioclase gneiss	113	biotite-quartz-plagioclase gneiss
51	heavy alteration	114	hornblende granitic gneiss
52	biotite-quartz-plagioclase gneiss	115	biotite-quartz-plagioclase gneiss
53	graphitic schist	116	biotite-quartz-plagioclase gneiss
55	biotite-quartz-plagioclase gneiss	117	charnockitic gneiss
56	biotite-quartz-plagioclase gneiss	118	biotite-quartz-plagioclase gneiss
57	mafic granulite	119	not certain
58	biotite-garnet-sillimanite gneiss	121	hornblende granitic gneiss
59	biotite-garnet-sillimanite gneiss	122	hornblende granitic gneiss
61	biotite-quartz-plagioclase gneiss	123	charnockitic gneiss (more granitic)
63	hornblende granitic gneiss	126	charnockitic gneiss (more granitic)
64	hornblende granitic gneiss	128	charnockitic gneiss (more granitic)
66	hornblende granitic gneiss	129	charnockitic gneiss
68	biotite-quartz-plagioclase gneiss	130	hornblende granitic gneiss
69	biotite-garnet-sillimanite gneiss	131	hornblende granitic gneiss
70	biotite-quartz-plagioclase gneiss	132	hornblende granitic gneiss
71	biotite-quartz-plagioclase gneiss	133	hornblende granitic gneiss
72	biotite-quartz-plagioclase gneiss	134	hornblende granitic gneiss
137	hornblende granitic gneiss	138	hornblende granitic gneiss